McGill University Department of Pharmacology
and Therapeutics

Bone-targeted Fluorogenic Probe for the Functional Imaging of Mineralized Tissues

Masters of Science Thesis

David McCusty
Supervisor: Dr. Bastien Castagner

Table of Contents

Abstract

Background

Bone remodelling is the process of degrading and rebuilding bone tissue. Uncoupling of this process results in disease, e.g. osteoporosis, or can occur as a result of other pathological processes, e.g. cancer metastasis to the bone. By detecting enzymatic cleavage by cathepsin K, the major protease involved in the breakdown of the organic collagen tissue in bone, it will be possible to monitor the activity of osteoclasts, a cathepsin K-expressing cell and the only cell capable of resorbing bone. This will be done using a fluorescent peptide probe sensitive to cleavage specifically by cathepsin K. To target the probe to bone, the bisphosphonates, a class of small molecule drugs that bind to the hydroxyapatite calcium mineral in bone, will be exploited. The bisphosphonate not only targets the probe to bone tissue but remains bound to bone after cleavage of the peptide substrate, allowing detection of the fluorescent signal after cleavage. Using this probe, and by changing the peptide amino acid sequence to be specific for additional proteases, a variety of proteases involved in bone processes can be studied.

Objectives

To develop and characterize with chemical and biological methods a Förster resonance energy transfer (FRET) internal peptide conjugated to the bone homing molecule alendronate, a therapeutic bisphosphonate. The probe will be used to monitor the activity of Cathepsin K expressed by osteoclasts cultured on a hydroxyapatite coated tissue culture plate.

Methods

The conjugation of alendronate to a fluorescent peptide was done in two steps. First, alendronate was conjugated to a maleimide moiety via formation of an amide bond. The product was

characterized by nuclear magnetic resonance spectroscopy. The maleimide-conjugated alendronate was then reacted with the fluorescent peptide, where the maleimide moiety conjugated to the sulfhydryl group of a cysteine residue. The fully conjugated alendronate-linked fluorescent peptide was characterized by LCMS. Fluorescence dequenching upon treatment with cathepsin K and other control enzymes have been performed in solution and on hydroxyapatite support to mimic the bone surface and measuring using a fluorescence plate reader or imaged with fluorescent microscopy.

RAW 264.7 cells, a mouse monocyte cell line, have been differentiated into osteoclasts on calcium phosphate coated culture plates. Fluorescence on the hydroxyapatite resulting from cleavage by Cathepsin K after addition of the probe will be imaged using fluorescence microscopy.

Results

Both steps of the probe synthesis have been successful, and the final alendronate-conjugated peptide has been purified to 85%. Cathepsin K has been shown to be able to cleave both the peptide and alendronate-conjugated peptide in solution. A model enzyme papain, cleaved the peptide-ale bound to a calcium phosphate surface. Osteoclasts grown on calcium phosphate plates resulted in an increased fluorescence after incubation with the peptide-ale.

Conclusions and Future Work

The probe in a purified enzyme model has shown fluorescence increase when dequenched via enzymatic cleavage as expected. This proof-of-principle model of cathepsin K in osteoclasts can be extended to cathepsin K in other processes, e.g. cancer metastatic to the bone and in pathological calcifications. By changing the peptide amino acid sequence, the basic probe

design can be extended to other proteases. *In vivo* imaging should also be possible using a similar design, if near-infrared fluorescence is used.

Preface

The experiments in subsection “Peptide Binding” were performed by Emmanuelle LeBlanc. The HPLC experiments in described in “Peptide-Linker Conjugated” were performed by Emmanuelle LeBlanc and Reem Kurdieh. Some replicates of the syntheses described in “Alendronate-Linker Conjugation” and “Peptide-Linker Conjugation” were performed as them as well. No conflict of interest is declared.

Introduction

Bones are a hardened, or mineralized, form of connective tissue. Composed mainly of the protein collagen and calcium phosphate minerals, they provide rigid support to the body and via their connections to skeletal muscles, tendons, and ligaments permit movement. The relative rigidity of bone compared to other tissues also gives it a protective function; for example, the brain is contained with the bones of the skull and the lungs inside of the rib cage, giving a degree of protection from trauma. Because a significant portion of bone is mineral, they also play an important role in the maintenance of mineral homeostasis, especially calcium. Bones also contain the bone marrow, which is primarily the site of hematopoiesis, the process of generating new blood cells, both erythrocytes and some blood cells of the immune system.

Bones are continually broken down and rebuilt in a process called bone remodeling. This process is critical to maintaining healthy bone, which is continually being stressed causing microfractures and loss of structural integrity of the tissue. Uncoupling of the process results in an imbalance of building and breaking down bone, a pathological state that can be caused by

many factors, including genetic conditions, environmental factors, diet and lifestyle choices, as a result of other diseases or an adverse effect of drug treatments. Two cell types are directly involved in the remodeling process: the osteoblasts that build new bone, and the osteoclasts that break down bone. Osteoclasts first break down bone and then are followed by osteoblasts which replace the resorbed tissue. This is known as the basic multicellular unit (BMU) [1].

Osteoclasts

Osteoclasts have a distinct morphology and are the only cell capable of breaking down bone tissue. The cells are a specialized multinucleated form of macrophages, formed by the fusion of monocytes. Osteoclasts are highly polarized, with an apical membrane facing the bone and a basolateral membrane on the other side where the cells are in contact with the vascular system. The apical membrane consists of a sealing membrane on the edge of the cell, which surrounds the ruffled border membrane on the inside, underneath the which the bone resorption activity takes place (Figure 1).[2] The sealing membrane consists of podosomes, foot-like structures where the cell attaches to the bone matrix. In a mature osteoclast, the podosomes are attached to an actin ring around the edge of the cell, another unique feature of the osteoclast. The ruffled border membrane comprises two major sections, the outer fusion zone, where vesicles from the cell fuse to the membrane to insert ion transporters and release lysosomal enzymes into the resorption pit, also called the resportion lacuna. The inner uptake zone takes up the bone breakdown products, and transcytoses them to the functional secretory domain on the basolateral side of the cell.[2] The area under the osteoclast, formed by the sealing membrane and ruffled border membrane, is known as the resorption pit or resorption lacuna. It can be thought of as a large extracellular lysosome, due to its acidic environment and high levels of proteases, many of which can also be found in lysosomes in other cells. And while the resorption pit is technically

extracellular because it is outside of the cell membrane, the sealing membrane prevents it from contact with most of the body, except for the bone surface and the osteoclast.

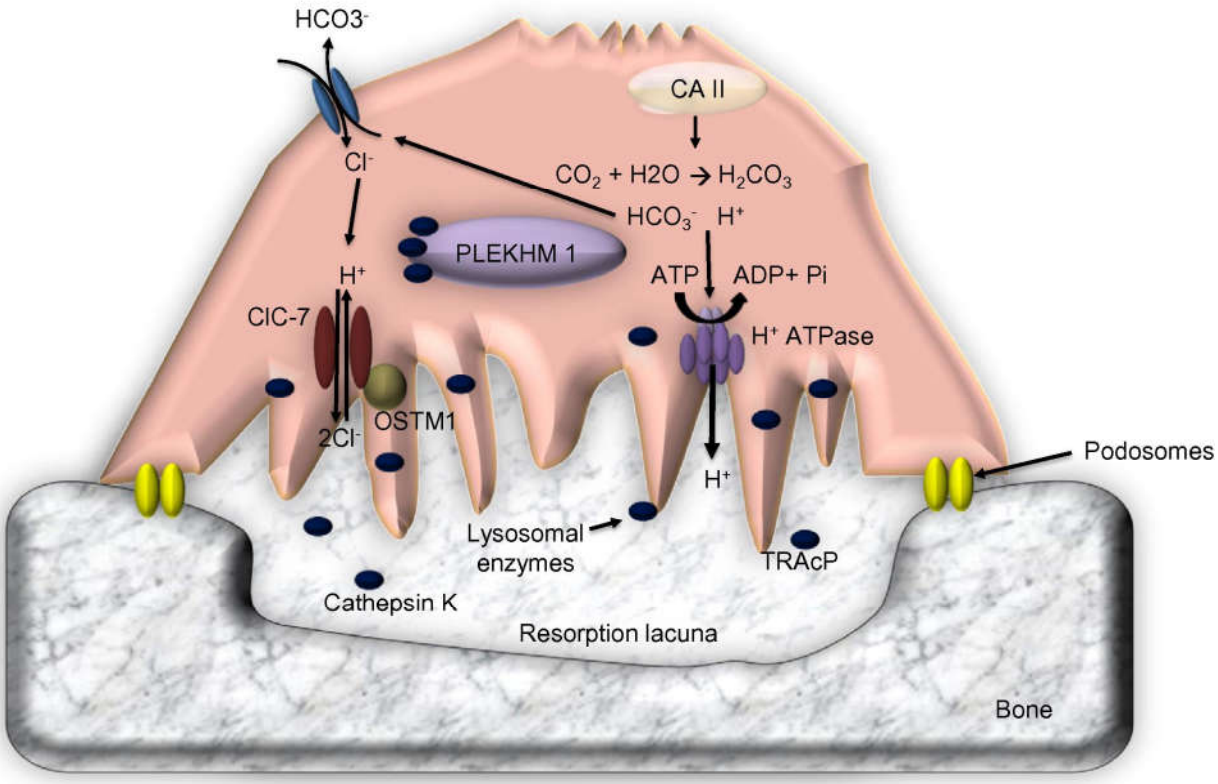

Figure 1 The mechanism of bone resorption. Cartoon depicting the molecular pathways involved in the acidification of the resorption lacuna and in the release of lysosomal enzymes, that disrupt both the inorganic and the organic bone matrix. Figure from Cappariello et al.[2]

The combination of the growth factor MCSF-1 (macrophage colony stimulating factor) and cytokine RANKL (receptor activator of nuclear factor (NF)-κB), which is related to TNF (tumor necrosis factor), act on monocytes to form osteoclasts. These are able to induce expression of genes typical of osteoclasts in the monocyte precursor cells, such as cathepsin K, tartrate-resistant acid phosphatase (TRAP), and β_3-integrin, which is necessary for mature osteoclasts to develop [3]. RANKL is also important to the regulation of osteoclasts; RANKL is a type II transmembrane protein expressed on the surface of cells including osteoblasts, which is

enzymatically cleaved and released in a soluble form, which is then able to bind to RANK expressing cells. RANK activates at least five different signaling cascades mediated by kinases: the inhibitor of NF-κB kinase (IKK), c-Jun N-terminal kinase (JNK), p38, extracellular signal-regulated kinase (ERK) and Src pathways. TRAFs, TNFR-associated cytoplasmic factors, bind to the cytoplasmic domain of the RANK receptor upon its activation. TRAF6 mutations result in osteopetrosis, a disease characterized by abnormally dense bone, as do RANK mutants that cannot bind TRAF6. TRAF6 assembles the signaling proteins that directly lead to osteoclast-specific genes, such as IRAK 1/3 which ultimately lead to NF-κB activation. It is important to note that that there is also a decoy receptor for RANKL known as OPG (osteoprogetrin); overexpression of OPG prevents the formation and activation of osteoclasts. OPG does not activate a signaling pathway of its own; it solely sequesters RANKL preventing it from binding to RANK. The expression levels of RANK and OPG control the activation and maturation of osteoclasts [4].

Osteoclast structure is closely related to their function. Osteoclasts resorb bone through two major processes– the creation of a highly acidic resorption compartment that dissolves inorganic minerals and degradation of organic material in bone, mostly type I collagen, through proteolytic enzymes. Acidification occurs by a relatively straightforward process; a V-type H^+-ATPase located in the outer fusion zone pumps protons out of the ruffled border membrane and into the resorption pit. To balance the electric charge of this process, a $2Cl^-/H^+$ antiporter brings a positively charged hydrogen ion into the osteoclasts and two negative chloride ions are pumped out of the cell into the resorption pit [5]. The intracellular proton source is for the proton pump is H_2CO_3, formed by carbonic anhydrase type II which hydrates carbon dioxide into bicarbonate. On the basolateral membrane, a Cl^-/HCO_3^- anion exchanger removes a bicarbonate ion,

preventing the pH of the cytoplasm from becoming too high after hydrogen ions are removed from the cell to acidify the resorption pit as well as bringing in a chloride ion to be pumped into the resorption pit by the $2Cl^-/H^+$ antiporter [2].

In addition to acidification, osteoclasts express high levels of proteases, lending them their ability to break down collagen. Cathepsin K is the most important and is involved in the breakdown of type I collagen, though other cathepsins such D, B, and L are also expressed. Matrix metalloproteinases are also highly expressed; MMP-9 is involved in the migration of osteoclasts across the bone surface [6] and in fracture healing and vascularization of the bone. MMP-2 is important in osteoclast development [7]. A number of other MMPs, including 3, 10, 12, and 13 are also found in osteoclasts though their function remains unclear, and may actually be produced by other cells, especially MMP-2 and -13 [8].

Cathepsin K

Cathepsin K is a potent collagenase and can break down type I collagen and elastin [9]. Combined with its high expression and localization into osteoclasts, it was becoming evident by the mid 1990s that cathepsin K is likely to be the key enzyme in the proteolytic breakdown of bone [10]. The identification of abnormal cathepsin K as the cause pycnodysostosis, a rare bone disorder characterized by dense, osteopetrotic bone prone to fracture, further supported the idea that cathepsin K is critical to the normal breakdown of bone [11]. Its structure is quite similar to other cysteine proteases, so its unique ability to cleave collagen's triple helix in multiple locations is mediated by subtle changes – a mutation of Y67L and L209A to mimic the amino acids found in Cathepsin L will knockout this ability – rather than large structural modifications [12]. Though other proteases, e.g. MMP-1, -8, -13 and -14 are capable of cleaving collagen's triple helix, cathepsin K is unique in its ability to do so in more than one location, mostly on the N-

terminal end though there is also a cleavage site on the C-terminal end. The extreme ends of the collagen molecule, termed the C- and N-telopeptides, can also be cleaved by cathepsin K and released from their crosslinks with adjacent collagen molecules. These terminal fragments can be used as markers of bone resorption activity. The wild type enzyme can cleave substrates with a proline at the P2 position, important due to the high proline content in collagen and a feature not found in other collagenases. Most other cathepsins prefer a hydrophobic residue in this position [13].

Bone Diseases

Osteoclasts, though necessary for maintaining healthy bones, are involved in diseases states and are a therapeutic target. Malfunction of the remodeling process can result in a number of diseases, though they are all characterized by weaker-than-normal bones. Osteopetrosis, literally meaning stone bone in Greek, is the formation of excessively dense bones, which tend to be brittle and prone to fracture. Pycnodysostosis is a rare form of osteopetrosis resulting from mutations in cathepsin K. Paget's disease of the bone is excessive remodeling; osteoclasts, which can be larger than in normal patients, break down bone in larger than normal qualities and the bone is rebuilt by osteoblasts. However, the bone forms in a disorganized manner resulting in weak bone. Osteopenia and osteoporosis are lowering of the bone density, with the former being less severe. Both are characterized by an excess of bone breakdown relative to the formation of new bone and are especially common in post-menopausal women due to lowered estrogen which both increases osteoclast activity and decreases osteoblast activity. Osteoporosis is also a concern with long-term use of glucocorticoids. Osteogenesis imperfecta or brittle bone disease is a heterogeneous group of disorders ranging from mild to lethal, though they are related by some protein malfunction related to bone, either in collagen itself or in collagen processing. All these

diseases occur on a spectrum of severity; mild forms may not even be noticed by the patient and are sometimes caught by screening tests including x-rays for other reasons. Serious forms result in pain, increased likelihood of fracture, and malformation.

Bone cancer is also a significant concern. Primary bone cancer is fairly rare, with all primary bone sarcomas representing only 0.2% of malignancies [14]. Bone metastasis is a greater concern and occurs at a much higher frequency. A survey of US adults estimated that 68% of secondary bone metastases come from a primary cancer of the breast, prostate, or lungs [15]. Since metastasis occurs in later stages of cancer, prognosis is poor. Treatment is largely palliative to reduce pain and discomfort to the patient. In the 19th century, English surgeon Dr. Paget described the "seed and soil" theory, where a tumor cell, the "seed", will only grow in a site amenable to its growth, the "soil". Though this theory has been expanded since, it is basically correct in that the microenvironment is important in where a tumor will metastasize, and bone is a choice location for at least some kinds of cancers. Another problem is that bone metastases initiate a "vicious cycle," in which the normal balance between resorption and deposition is disrupted, and there is a feedback cycle resulting in either excessive bone breakdown or deposition. The cancer cells produce their own signaling proteins that effect change in the normal feedback. [14]

Treatment of Bone Diseases

There are several treatment options for bone disorders. Many are not pharmacological and involve diet and lifestyle changes. Physical therapy can be used to help strengthen bones and muscle. Assistive devices like crutches and wheelchairs are also used. Surgery can insert rods to take stress off the bones. Pharmacological agents that strengthen bone, usually by inhibiting resorption are also used. These drugs are frequently used with calcium and vitamin D

supplementation. Denosumab is fully human antibody to RANKL, resulting in lower levels of RANKL and therefore lower levels of osteoclastogenesis. It is somewhat similar to the endogenous protein osteoprotegrin (OPG) in that its mechanism of action is to prevent RANKL binding to RANK. Specific inhibitors of the protease cathepsin K have been developed, though none are currently approved for therapeutic use. It bears noting that alendronate, and the rest of the bisphosphonates, do not target cathepsin K directly. Since cathepsin K is the primary enzyme involved in breaking down, and is only expressed in low levels elsewhere, it would seem that a cathepsin K inhibitor would be effective in increasing bone mineral density with relatively few adverse effects.

This is rather difficult in practice, however, because there are many other cathepsins (for example B, L, and S) that are structurally very similar. And because these enzymes are found in acidic lysosomes, a lysosomotropic drug is not good as the drugs would have a locally increased concentration and increased side effects on other cathepsins. Additionally, the drug has to be metabolically stable for a reasonable period of time, and ideally not subject to CYP enzymes that are induced or inhibited by common drugs or food. After changing side chains of a lead compound to enhance selectivity and potency, a drug called odanacatib was developed, with on- and off-rates of 5.3 x10^6 $M^{-1}s^{-1}$ and 0.0008 s^{-1}. [16]. Unfortunately, Merck did not decide to license and market the drug after an elevated risk of stroke was found after round three clinical trials [17]. The drug doses used in cancer treatment are nearly always much higher than those used for Paget's disease and osteoporosis. The most common drugs, however, are a class of drugs known as the bisphosphonates, which inhibit osteoclast activity therefore reducing the breakdown of bone.

Bisphosphonates

Bisphosphonates sequester well into bone tissue by binding to the inorganic calcium matrix of bone tissue. Bisphosphonates, including alendronate, have very low oral bioavailability in serum, often less than 1%.[18] This is a result of their negatively charged phosphate groups, hydrophilic nature, and the formation of calcium complexes in the GI tract that are difficult to absorb. However, they strongly chelate calcium, and as a result about half of the bioavailable bisphosphonate binds to skeletal tissue. Bisphosphonates like alendronate that have a hydroxyl group on the central carbon form a tridentate bond with calcium; those without a hydroxyl group form a bidentate bond. Any unbound drug is excreted without being metabolized by the kidneys. It has been shown, using radiolabeled drugs, that bisphosphonates preferentially bind to active resorption sites.[18] Some of the drug also binds within the bone where it is embedded and believed to be biologically inert; only the drug that binds to the bone surface exerts a pharmacological action. Furthermore, it is possible for the drug to be released by an osteoclast and then rebind to the bone, exerting its action multiple times.[18] Though it is difficult to measure because alendronate lacks a chromophore and the strong polarity makes it difficult to separate from biological samples, it is believed that the skeletal half-life of alendronate is about ten years, as opposed to less than two hours in serum [18].

Pharmacodynamically, the nitrogen-containing bisphosphonates inhibit farnesyl pyrophosphate synthase (FPPS), part of the mevalonate synthetic pathway. More specifically, FPPS prenylates small GTP-binding proteins. Inhibition of this process results in disruption of the cytoskeleton, which interferes with the ability of the osteoclast to create the sealing membrane and ruffled border membrane, without which they cannot properly function. Since the drugs bind specifically to the calcium phosphate in bone, it is released by osteoclast bone-resorbing actions and has little effect on any other cells [19]. It is interesting to note the mechanism

of action of alendronate was not fully elucidated until 1998,[20] after the drug had entered clinical trials. The drug was approved by the FDA under the brand name Fosamax on November 24, 1999.[21]

Side Effects of Bone Treatments

Side effects for the various pharmacological treatments are similar. Some are common to many drugs, like nausea and indigestion and pain at the site of injection. The most serious concern with anti-resorptive drugs is osteonecrosis of the jaw, a painful condition where the jaw bone is exposed through the gums with lesions that do not heal due to a lack of blood supply. It usually results from trauma, for example after dental surgery, though spontaneous development is possible. It is difficult to treat, and many treatment strategies focus on reducing risk of infection rather than actual treatment of the necrotic tissue. The mechanism of action is not known, and it is also not known why this effect is unique to the jaw, though it likely is related to a reduced ability of the bone to heal because the normal remodelling process has been inhibited by the anti-resorptive treatment. The effect is very rare at the doses of any drug, including the bisphosphonates and denosumab, used for osteoporosis; it is seen almost exclusively in the much higher doses used for cancer treatment [22].

Other Uses of Bisphosphonates

Though the main use of bisphosphonates is treatment of bone diseases as described above, their calcium-binding properties have led to investigation into other uses. After the opening of a blocked vein or artery by angioplasty, there is a risk of thickening of vessel tissue. Bisphosphonates have been shown to deplete circulating white blood cells, like leukocytes, an effect that is enhanced by encapsulation in liposomes,[23] which reduces the risk of thickening of the vessel tissue. Bisphosphonates can be used in a similar way as anti-tumor agent;

encapsulation into liposomes or nanoparticles enhances uptake into phagocytic cells or increases their deposition at tumors.[18] By depleting macrophages associated with the cancer, TNFα (tumor necrosis factor alpha) is reduced, increasing the efficacy of radiotherapy.[24]

Failure of implants to adhere to bone is a major source of failure in orthopedic surgery.[25] This is often a result of an inability of the implant to stabilize due to resorption of the supporting bone. By coating the implant in bisphosphonates, attachment to the bone is enhanced by reducing bone loss.[25] Bisphosphonates could also be used in conjunction with antibiotics on the implant surface to reduce osteomyelitis, which is a bone infection resulting in bone destruction and loosening of the implant.[25]

Bisphosphonates have also been used to target other drugs to bone, exploiting their bone-binding properties. Conjugation of estradiol, which increases bone mass but has several side effects including increased cancer risk, via an ester bond to a bisphosphonate reduced bone loss in ovariectomized rats. Radionuclides are known to reduce pain from cancer metastases, and conjugation to bisphosphonates targets the radionuclides to bone with little uptake in other tissues. Another technique is to conjugate a chemotherapeutic agent, which can then bind with the bisphosphonate to bone and be released by hydrolysis. A similar strategy can be used with antibiotics for osteomyelitis, which is usually difficult to treat and involved a combination of surgery and antibiotic treatment.[25]

Bisphosphonates have also been used as imaging agents. As described above, conjugation to a radioisotope is used clinically for imaging. However, this technique requires long scan times of approximately half an hour as well as limited resolution; as the field of view gets larger, the resolution decreases.[26] An alternative method using conjugation of a near-infrared dye to a bisphosphonate, specifically pamidronate, has been used.[26] Near infrared dyes provide a great

advantage over dyes in the visible spectrum, because autofluorescence of tissues is low in this range, from 700 to 900 nm and penetration of the photons is high. The major advantage of a system like this over using radioisotopes is that the resolution is much higher, especially at bony structures near to the skin. For example, it is possible to see the maxilla with almost photographic clarity, as opposed to the somewhat blurry imaging that results from a bone scan image. This increased resolution gives the potential to see cancer metastases before they become symptomatic or visible by other imaging techniques.[26] Zaheer et al. suggest it would also be possible to visualize coronary calcification in its earliest stages, again because of the increased resolution. This even has "theranostic" potential, where the calcification could be imaged and treated by the same compound when combined with photodynamic therapy. This technique is limited in its ability to image deep structures. Even though using NIR dyes over dyes that fluoresce in the visible range reduce scattering and signal attenuation, there is still more loss of signal than with the traditional radioimaging, which remains better for imaging deeper structures, but it lacks the resolution possible with NIR dyes.[26]

Bone Imaging

The simplest form of bone imaging is the x-ray, which is useful in imaging large fractures and some metastases. However, it is not a particularly sensitive technique and may miss smaller pathologies, which is to say it has a high rate of false negatives. To overcome this limitation, nuclear medicine was used. A bone scan, also known as bone scintigraphy, is a much more sensitive technique and is useful after a negative plain x-ray. This technique uses a radioligand that binds to bone, most commonly ^{99m}Tc in complex with methylene disphosphonate, which is the simplest bisphosphonate (i.e. two phosphate groups bound to a central carbon with no other side chains). Because bisphosphonates bind preferentially to where bone is actively being

remodeled, the complex localizes to sites of injury, e.g. fracture, and cancer metastases. The radiation from the ^{99m}Tc methylene disphospohonate complex can then be imaged with a gamma camera. This is useful in the clinic as a diagnostic technique for both malignant and non-malignant skeletal diseases, however, it contains little information as to what is happening at the molecular level.[27]

Fluorogenic Probes

Fluorogenic probes are widely used in molecular biology. The basic principle of fluorescence is that some molecules are able to absorb a photon and change to a singlet excited state. There is then a relaxation to the first singlet excited state, and then upon return to the ground state a photon is released. Because there is a loss of energy in the relaxation to the first singlet excited state, the released photon is at a lower energy than the absorbed photon. The difference in the maximum excitation value and the maximum emission value is known as the Stokes shift; the emitted photon is lower energy and therefore longer wavelength than the emission photon. [28]

Generally speaking, the redder a fluorescent dye is the better its use for biological imaging. Dyes fluorescent in the near infrared range, from 700 to 900 nm, are less affected by autofluorescence and photon scattering than dyes more in the visible range.[29] However, these dyes are much more expensive and not necessary for all applications.[29] High autofluorescence in scattering in the visible range means that dyes that fluoresce in this area are of a little to no use in live animals, though they can still be useful in cell-based assays and for dissected animals.

Fluorescent probes find a myriad of uses in fluorescent biology. Fusion of a fluorescent protein onto a protein of interest allows for imaging of a specific protein, giving information like where and when it is expressed and how it responds to various stimuli. Conjugation of

fluorescent dyes onto antibodies allows for immunohistochemical imaging, showing where a protein or cellular structure is located without the need for a genetically modified organism with a fusion fluorescent protein. The two methods can also be combined, for example with a green fluorescent protein (GFP) tagged protein and then another fluorescent antibody that labels the cytoskeleton. Fluorophores in general are also sensitive to photobleaching; eventually their fluorescence is permanently lost, and it cannot be recovered.

Fluorophores can also be used for purposes other than imaging. For example, flow cytometry can analyze and separate individual cells in a population based on their fluorescence. This can be used to separate cells expressing a fusion fluorescent protein, for example a progenitor cell that expresses a certain protein not found in the mature cell. Microplate readers measure the average fluorescence of a sample, without regard to exactly what is going on in an individual cell.

Alendronate-Conjugated Probe for Cathepsin K

The basis of this project is to create a novel investigative agent to study bone and its remodeling in a novel way beyond current clinical techniques like x-rays and bone scans and lab techniques like Western blotting and immunohistochemistry, though our technique could be combined with these methods. By using a bone-binding drug, namely the bisphosphonate alendronate, we can create a probe that will bind and remain bound to the calcium phosphate mineral giving better spatial and temporal resolution than previous probes because the probe stays bound to where it was cleaved. This means that it is possible to look at longer time periods, potentially weeks depending on the stability of the fluorophore because the probe will not diffuse away from the site of interest. The design is based on static quenching consisting of a dye-

quencher pair linked by amino acid sequence (see figure 2). Fluorescence increases upon physical separation of the dye and quencher pair from cleaving of the amino acid sequence.[30] The amino acid sequence can be changed to made specific to various enzymes, but as a proof-of-principle the amino acid sequence is specific to Cathepsin K. The dye and quencher choice was made in conjunction with the supplier, BioBasic Inc., as well as a literature search that the pair did in fact have a reasonable quenching efficiency.[31]

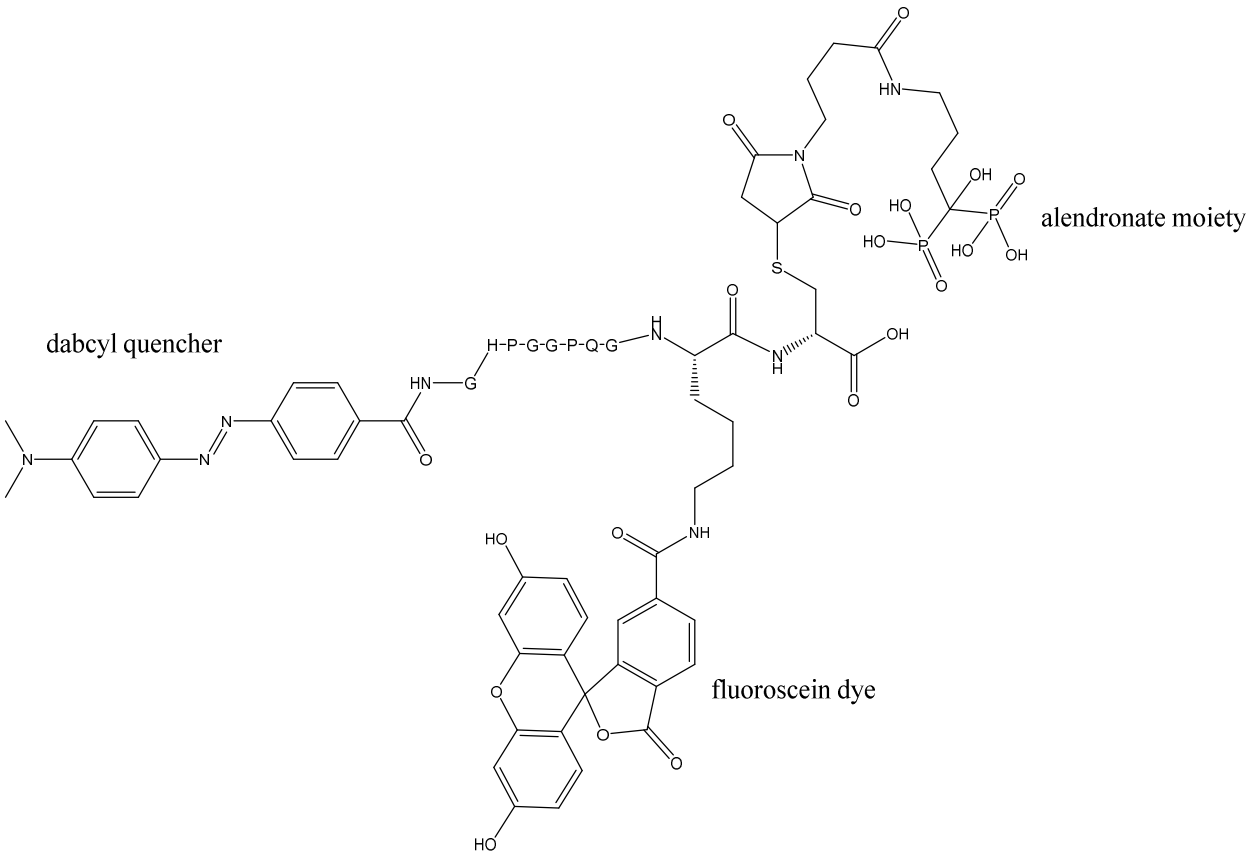

Figure 2 The molecular structure of the fluorescent probe. A peptide conjugated to the fluorescent dye fluorescein is quenched by dabcyl and linked by a peptide sequence. Upon cleavage of this sequence, the dye and quencher are physically separated, and the dye is able to fluoresce freely. The alendronate facilities binding to calcium phosphate and keeps the dye bound to the calcium phosphate as well.

Our probe exploits the pharmacokinetic properties of the bisphosphonates. Since the bisphosphonates bind to calcium phosphate strongly and specifically, it is possible to use bisphosphonates as a targeting moiety for a probe. We base our probe on a similar probe that has

been previously used to image calcified atherosclerotic plaques [32], where Cathepsin K is known to be involved in destabilization of the plaques which can result in adverse cardiovascular events including heart attack and stroke. However, the previous probe lacks a targeting moiety, the addition of which we hypothesize will improve the temporal and spatial resolution of the probe because it will not diffuse from the site of cleavage. Additionally, at time of writing, there are no commercially available antibodies able to distinguish cathepsin K from its inactive proenzyme form. Though migration distance changes in electrophoresis due to size differences, there are not currently antibodies available that can distinguish the two forms in an immunohistochemical setting. Our probe shows the location of enzymatic activity, which was suggested by Jaffer et al. to not always be identical to where cathepsin K is found by immunostaining, i.e. not all of the immunoreactive cathepsin K was enzymatically active.[32]

The Jaffer et al. probe is peptide based, with a Förster resonance energy transfer model composed of an internally-quenched fluorescent dye conjugated to a polymer via the peptide amino acid sequence of G*HPGGPQ*GKC-NH_2. The italicized amino acids indicate the core sequence, already known to be specific to Cathepsin K by the work of Lecaille.[30] The Lecaille et al probe is also a FRET-internal peptide-based probe, specifically Abz-HPGGPQ-EDN_2ph. Abz and EDN_2ph are *o*-aminobenzoic acid and *N*-(2,4-dinitrophenyl)-ethylenediamine respectively, acting as a dye and quencher pair.[30] However, this probe lacks the bone-binding ability afforded to ours by the addition of alendronate though it maintains the stimulus-response nature in that cleavage increases the fluorescence signal. Upon cleavage of the peptide, the dye and quencher are physically separated, and the quencher no longer prevents the fluorescence of the dye resulting in a fluorescence increase upon enzymatic cleavage.

Our probe uses the combination of fluorescein and dabcyl is a reporter and dark quencher pair. Upon excitation of fluorescein by absorption of a photon, the dabcyl prevents the fluorescein from being able to go to a lower energy state by radiation, i.e. emission of a photon resulting in fluorescence, and the dye instead transfers its energy to the quencher, which then releases the energy as heat. The use of a dark quencher over some other quenchers, e.g. TAMRA, is that they are not able to fluoresce on their own. Since there is no fluorescence of the quencher when using dabcyl, background is reduced, and the signal-to-use ratio is improved.

Cathepsin K Selective Sequence

This cathepsin K specific peptide sequence had been previously identified as a substrate of congopain, a protease from *Typsonosoma congolense,* which causes an animal disease known as nagana similar to African sleeping sickness in humans. In order to verify that the sequence is in fact specific to Cathepsin K, Lecaille et al. determined that cathepsins B, F, H, L, S, and V, as well as the Y67L/L209A Cathepsin K mutant were unable to cleave it. Fibroblast lysates from mice were able to cleave it, but lysates from Cathepsin K-deficient samples were not, strongly indicating that this sequence is specific to Cathepsin K among mammalian proteases.[30] So while there are enzymes other than cathepsin K that can cleave the substrate, they are not found in mammals.

Our probe uses an amino acid sequence identical to the Jaffer et al. probe, G*HPGGPQ*GKC-NH2 (cathepsin K core sequence italicized,) with a dabcyl quencher moiety conjugated to the N-terminal glycine, and a fluorescein (FITC) fluorescent dye conjugated to the primary amine of the side chain of the lysine residue. Our key modification of the probe is the addition of a bisphosphonate targeting moiety, specifically alendronate. The alendronate is linked via a maleimide moiety to the sulfhydryl of the C-terminal cysteine. Because of the

presence of the dabcyl quencher, fluorescence is low when the peptide substrate is uncleaved. When cleaved by cathepsin K, the dye and quencher are separated and fluorescence increases. The key advantage of using the bisphosphonate targeting moiety is that the alendronate and fluorescein fluorescent dye remain on the same portion of the cleaved peptide, meaning that fluorescence should be visible where the cleavage occurred on the surface of the bone without diffusing away. Since the design does not involve the use of antibodies or recombinant fluorescent proteins, it can be used on live cells, fixed cells, or animals without the use of antibodies or the creation of transgenic animals.

We plan to synthesize an alendronate-conjugated cathepsin K sensitive probe that is able to bind to the calcium phosphate in bone and be cleaved by cathepsin K. This will involve three major sets of experiments: the chemical synthesis and analysis, biochemical assays, and biological assays and *in vitro* cell culture imaging. The probe will be synthesized and verified using NMR and mass spectrometry. We will then use purified enzyme assays to ensure that the probe can be cleaved, and we will perform experiments to indicate binding to calcium phosphate. The probe will then be used in a cell culture model of osteoclasts.

Materials and Methods

Alendronate-Linker Conjugation

A solution of non-buffered 7.2mg alendronate sodium trihydrate (TCI America) was made in 600 µL of water for concentration of 37 mM and adjusted to pH 10 using 1 M NaOH. Additionally, a solution of 4.3 mg 4-Maleimidobutyric acid *N*-hydroxysuccinimide ester (Sigma-Aldrich) was dissolved in 600 µL acetonitrile for a final concentration of 25.6 mM. The two solutions were added to a 10 mL round bottom flask. After 10 minutes, pH was checked and if

the solution was still basic HCl was added to neutralize it. If the solution was acidic, no pH adjustment was done. The acetonitrile was removed on a rotary evaporator (Büchi) at room temperature and a pressure of 85 mbar. The remaining aqueous solution was added to a charge Strata C-18 reversed-phase column (1g, 70Å, Phenomenex), which had been equilibrated twice with 10 mL of methanol (Fisher Scientific) and three times with 10 mL of water. Ten fractions of 1 mL each with water as the mobile phase were eluted, collected, then frozen at -80℃, and lyophilized at -90℃ and 0.010 mbar pressure (Christ Alpha 2-4LDplus). One-dimensional NMR data was then collected (300 MHz, in deuterium oxide, Varian).

Peptide-Linker Conjugation

The molar ratio of this conjugation is 5:1 alendronate-linker, described above, to avoid having leftover peptide, dabcyl-GHPGGPQGK-(5,6-fam)-C-NH_2 (custom synthesis by BioBasic in Markham, ON). 2.7 mg of alendronate linker was dissolved in 1 mL of 0.1M sodium phosphate, 0.15M NaCl, 0.1M EDTA, pH 7.2 buffer.[33] 2 mg of dabcyl-GHPGGPQGK-(5,6-fam)-C-NH_2 peptide in 50 µL of N,N-Dimethylformamide (DMF) was added to the alendronate-linker containing solution and allowed to react for two hours with shaking at room temperature. This solution was purified on a PD10 desalting size-exclusion column (GE Life Sciences) eluting with 10% acetonitrile in water with 0.1% trifluoroacetic acid. The orange-colored fractions, indicating the presence of the fluorescein dye, were frozen and lyophilized.

The fractions and then analyzed by reversed-phase high performance liquid chromatography (Agilent) equipped with an XSELECT® CSH C18 5.0 µm column (3.0 mm × 150 mm). The mobile phase gradient started with 70% water and 30% ACN, both containing 0.1%TFA at a flow rate of 0.425 ml/min. The percentage of ACN increased to 100% over 15 minutes, where it stayed constant for an additional 5 minutes. UV absorbance was measured at

280nmFractions with clean peaks were frozen, lyophilized, and stored at -80°C. Fractions were weighed and purity calculated, using the ratio of integral of the 6.6 min peak to the peaks for impurities. Using the same method but adding the peptide not linked to alendronate, a peak corresponding to the plain peptide was observed at 15.2 minutes.

Substrate Fluorescence

Procathepsin K (Enzo Life Sciences, ALX-201-239-C010) was activated according to manufacturer instructions. The stock enzyme was incubated at 37º for forty minutes in equal volume of 100mM sodium acetate 10mM DTT, and 5mM EDTA pH 4.0 solution. The enzymatic activity was confirmed using the omnicathepsin fluorogenic substrate, Benzyloxycarbonyl -Phe-Arg-7-amino-4-methylcoumarin (Enzo Life Sciences, data not shown) before beginning experiments with our custom synthesized substrates.

Assays were performed in a 96 well black polystyrene plate (Brand). The assay buffer is 50mM MES, pH 5.5, containing 2.5mM EDTA and 5mM DTT. 200 µL of buffer are added to each well and allowed to sit in the plate reader (Tecan Sparc 10M to warm to 37º. Peptide and peptide-ale are added to each well for a final working concentration of 13 µM. A baseline fluorescence read is taken in order to be able to normalize values. Then, either papain (1 µL of a 40 µM solution), activated Cathepsin K (1 µL of a 2.1 mM solution), or no enzyme (1 µL of FBS) are added and the plate is incubated with fluorescence reads taken every 10 or 15 minutes.

Additionally, the commercial peptide was incubated with MMP-9, matrix metalloproteinase-9 (Enzo Life Sciences ALX-200-422-C005), another enzyme important in osteoclast activity. MMP-9 was activated by incubation at 37°C for 40 minutes in the manufacturer recommended buffer of 50mM HEPES, 10mM $CaCl_2$, 0.05% Brij-35, pH 7.5 and

assayed using the same buffer. Activation was confirmed using an MMP fluorogenic substrate (Enzo Life Sciences).

Calcium Phosphate Plate Creation

96-well polystyrene plates were coated using simulated body fluid, which is three separate solutions made to 2.5x physiological ion concentration. The tris solution is 50 mM Tris HCl adjusted to pH 7.4. The calcium solution is 25 mM calcium chloride, 1.37 M sodium chloride and 15 mM magnesium chloride dissolved in the tris solution and adjusted to pH 7.4. The phosphate solution is 10 mM sodium phosphate and 42 mM sodium bicarbonate again dissolved in the tris solution and adjusted pH 7.4. Just before adding to the plate, the three were mixed together in a 2:1:1 ratio of tris:calcium:phosphate solutions. The SBF solution is then filtered with 0.2 polyethersulfone μm syringe filter (VWR). 100 μL of this calcium phosphate solution is added to each well of a 96 well plate using a multichannel pipette. The plates are then incubated covered and refrigerated 4 ℃. Every day for three days the solution is removed, and fresh 2.5 SBFx solution is mixed, filtered, and added to the plate.

On the third day, a different calcium phosphate solution of 2 mM sodium phosphate, 4 mM calcium chloride, 137 mM sodium chloride, and 50 mM Tris was made, adjusted to pH 7.4, and added to the wells previously coated with SBF. Incubation was for twenty-four hours at 4 ºC covered in a refrigerator. The solution was then removed, the plates were rinsed with distilled water and sprayed with ethanol to dry. Because the plates are made in non-sterile conditions, they were twice sprayed with ethanol and allowed to dry in a sterile culture hood with the UV light on before use.

Peptide Binding

0.5 mg each of the commercial peptide and the peptide-ale were diluted in 0.5 mL DMF and 200 µL HEPES buffer. 20 µL of this solution was then diluted 10x by adding it to 180 µL of HEPES buffer. 20 µL of the solution only containing plain peptide was then diluted by placing it into 5 µL DMF and 200 µL HEPES buffer.

60 mg of the calcium phosphate mineral hydroxyapatite (BioRad) were suspended in 3 mL of HEPES buffer. The suspension was stirred vigorously, and 50 µL were removed and added to both the plain peptide and peptide-ale solutions. These solutions were then shaken for 30 seconds and centrifuged for 30 seconds. 30 µL of supernatant were added to a clear 96 well plate (Brand) containing 170 µL HEPES buffer. The suspensions were then returned to the shaker and shook for 5, 15, and 30 minutes with centrifugation and 30 µL removed and added to 170 µL of HEPES solution in the 96 well plate. Absorbance was measured at 495 nm, the peak for fluorescein, in the Tecan plate reader. Fluorescence was not used here due to the quenching of the peptide. 200 µL of HEPES buffer was used as a blank and subtracted from absorbance values. These plates were imaged using the Operetta High Content Imaging system (Perkin Elmer), which was also used for cell culture imaging.

Cell Culture

RAW 264.7 mouse monocyte cell line (ATCC) were cultured in DMEM (Dulbecco's modified eagle medium) with 10% FBS (Fetal Bovine Serum) and 1% penicillin/streptomycin (all from Wisent). 50 ng/mL of recombinant human RANKL, receptor activator of nuclear κB ligand, produced in *E. coli* was added to the media (Peprotech 310-01). Cell density was 6000 per cm^3, or 2000 cells in a 0.33 cm^3 96 well plate. On day two of culturing, media was changed. For a negative control of RANKL-primed cells that do not form osteoclasts, the new media does

not contain RANKL. For osteoclast formation, RANKL was again added to the media at 50 ng/mL. Osteoclast formation occurred after 4-6 days and was indicated by the presence of large, multinucleated cells, a significant morphological change from the mononucleated monocyte precursor cells.[34]

Fluorescence

After the formation of large multinucleated cells, peptide-ale was added to three wells of monocytes and three wells of osteoclasts and given twenty-four hours to incubate. The next day, peptide-ale is added to three wells of monocytes and three wells of osteoclasts for a negative control and given 5 minutes to bind. Cells are then fixed with 10% neutral buffered formalin for 5 minutes. DNA is stained with Hoechst 33258 (Thermo Fisher) at 80 μM in PBS (phosphate-buffered saline, pH 7.4) for five minutes, washed three times with PBS, wrapped in aluminum foil and stored at 4℃.

Imaging

Fixed cells were imaged using an Operetta (PerkinElmer) high-content screening fluorescence microscope. Cells were imaged with a Hoechst filter (main excitation: 380 nm, main emission: 445 nm), FITC filter (main excitation: 500 nm, main emission: 560 nm), and brightfield. Images were then quantified using the Columbus (Perkin Elmer) analysis software. Intensity of FITC brightness for the whole image and a nuclei count were performed. Each plate had 3 wells per condition, and eight plates were imaged for a total of n=8 with three technical replicates each.

Results

Alendronate-Linker Conjugation

The bone-binding drug alendronate was first linked to a maleimide moiety. Secondly, the alendronate-maleimide was linked via a cysteine residue on the fluorescent peptide to afford the final peptide-alendronate product. Success of the first step, the conjugation of alendronate to the maleimide via formation of an amide bond, was measured with ^{1}H-NMR. A sample is shown in Figure 3. A major shift occurs on the hydrogens on the carbon alpha to the amine in alendronate, marked with e" and e and highlighted in green. The size of the peaks can be integrated and compared to show much alendronate-maleimide was formed compared to alendronate. There is also a possibility in basic conditions that the ester will hydrolyze, leaving a maleimide with a

carboxylic acid group attached. This is seen with the a', b', and c' peaks. It is also possible the maleimide itself can hydrolyze, however this was never observed.

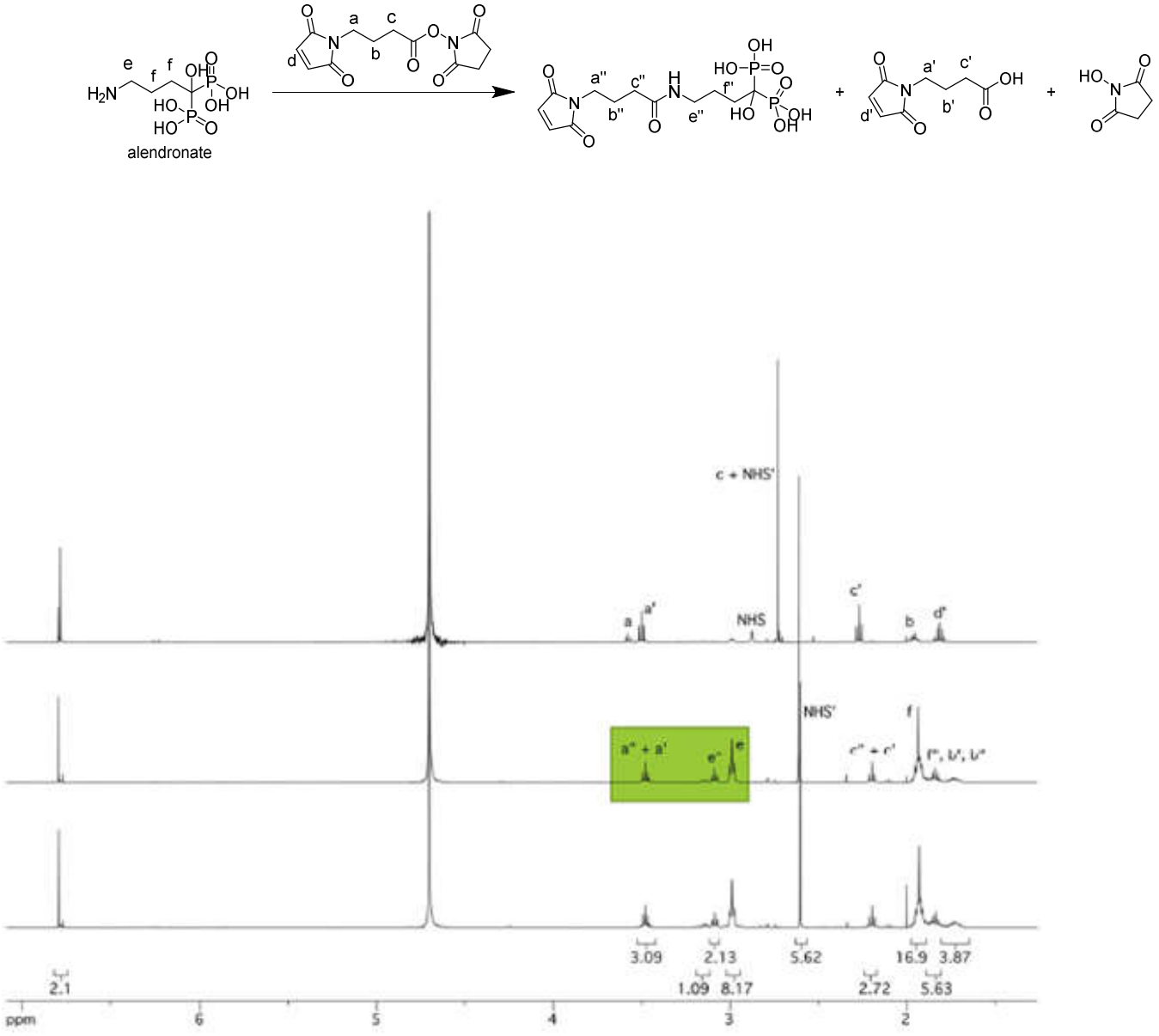

Figure 3 Sample annotated NMR spectra and synthesis of the alendronate-maleimide linker. Major shift of the hydrogens on the carbon alpha to the amine group of alendronate after conjugation to the maleimide and formation of amide bond marked with e and e" and highlighted in green. The combination of a" and a' also marked in green indicates an impurity resulting from ester hydrolysis. The three spectra are from collected 1 mL fractions 3, 4, and 5 from the top down.

However, this NMR spectrum shows the presence of impurities. This first synthesis attempt was alendronate tetrabutylammonium salt dissolved in dimethylformamide, in which it is soluble to approximately 15 mg/mL, which was added to 4-maleimidobutyric acid N-

hydroxysuccinimide ester dissolved in water in an equimolar concentration. The mixture was shaken overnight at room temperature in a plastic Eppendorf tube. The solution was then transferred to a scintillation vial where 2 mL of water and 5 mL of dichloromethane was added. The organic solvent was then removed. A C18 solid phase extraction column was charged with methanol twice and then rinsed four times with water. The reaction mixture was then added to the column. Eight fractions of 1.5 mL each were eluted with water. The fractions are then frozen and lyophilized. 1D H-NMR (Varian 300 MHz) were taken. A C18 column is charged and used again if NMR data indicated the presence of impurities.

Since this method did produce the desired product but was difficult to purify, we also attempted to use LH20 (Sephadex, Sigma-Aldrich) size exclusion column, but to no avail. We then attempted to use hydrophobic triethylammonium acetate buffer in conjunction C18 column in order to retain the bisphosphonate salts better on the reverse-phase material, but this also did not result in pure product.

After changing the protocol to that described in the methods section, where the conjugation of alendronate sodium to the maleimide was done under basic conditions and purified with a C18 column, it was possible to obtain the alendronate-maleimide linker where there were no starting reagents or side products other than NHS. Figure 3 shows the annotated NMR spectrum of a purified fraction using reverse-phase chromatography. The shifts found correspond to the protons found in the alendronate-maleimide linker; δ 6.87 (s, 2H), 3.56 (t, J = 6 Hz, 2H), 3.17 (t, J = 6 Hz, 2H), 2.28 (t, J = 6Hz, 2H), 1.97–1.89 (m, 4H),1.84–1.77 (m, 2H).

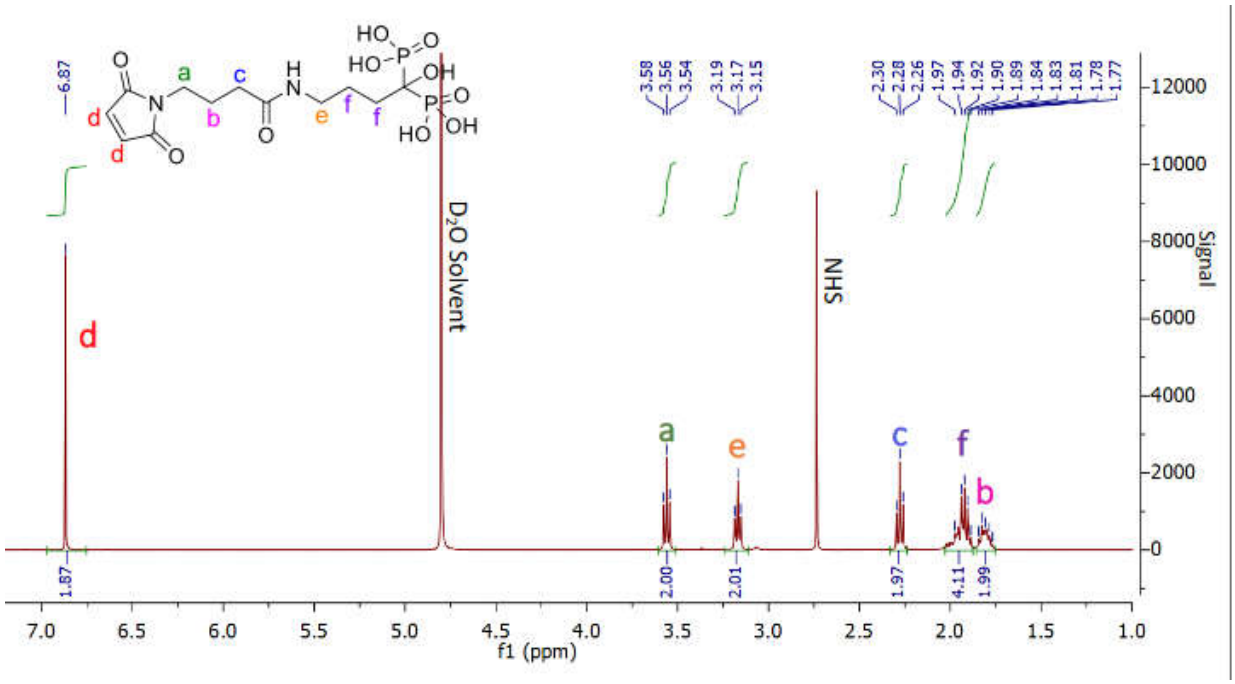

Figure 4 Annotated [1]H NMR spectrum of Alendronate maleimide linker confirms its presence and purity where all the peaks (labeled by small letters) are related to the hydrogens found in the product; The peak of D_2O solvent and NHS are shown as well.

Peptide Conjugation

The crude peptide conjugation reaction was analyzed by LCMS using a reverse-phase XSELECT® CSH C18 5.0 µm column (3.0 mm × 150 mm) column and a 0-100% ACN in water containing 0.1% TFA gradient. A chromatographic peak eluted from the LC column at 6.6 min, as seen in the 280nm absorbance HPLC trace in figure 5. The corresponding mass spectrum shows the mass-to-charge ratio values $[M + 2H^+]$ = m/z 980.6, $[M + 3H^+]$ = m/z 654.1 and $[M + 4H^+]$ = m/z 490.8 which are very close to the expected m/z values of the conjugated peptide (Molecular weight 1958.75): 980.4, 653.9 and 490.7, respectively, indicating that this peak corresponds to our desired product. Consequently, by integrating the peaks found in the UV-absorption spectrum, the coupling reaction and subsequent LC purification resulted in 85% pure probe.

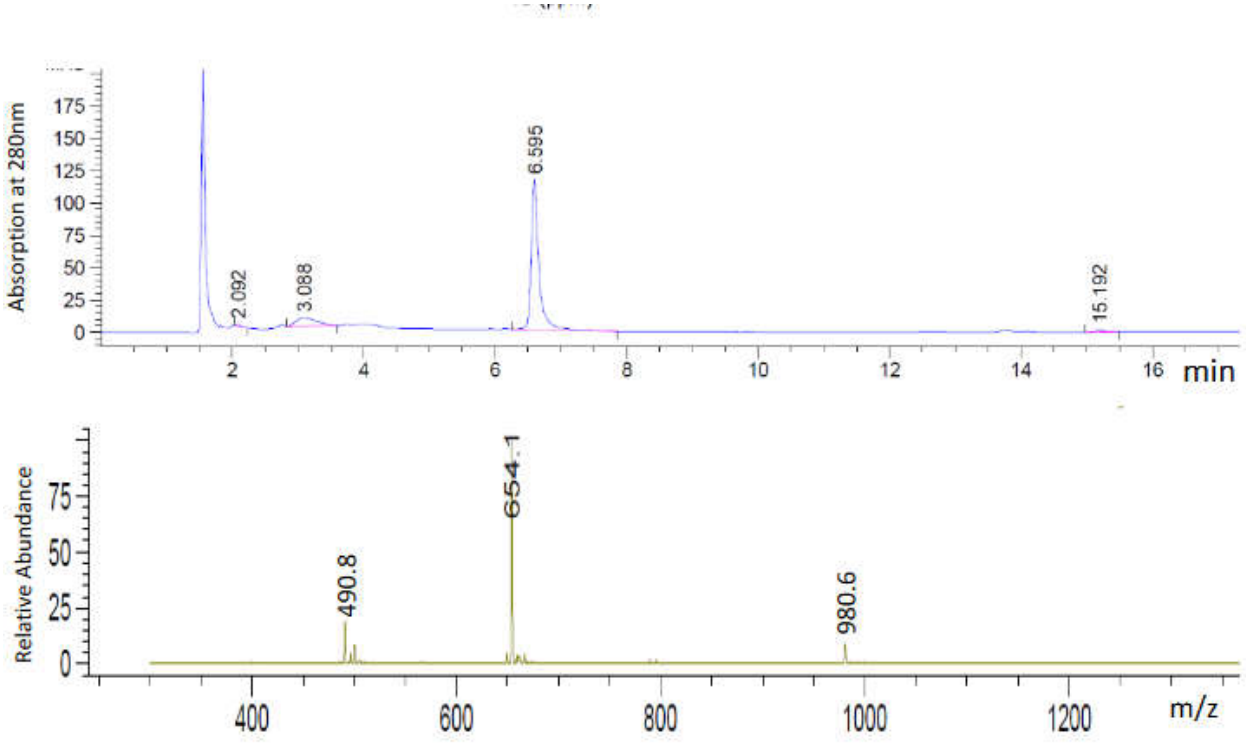

Figure 5 Liquid chromatography spectrum, at 280nm absorbance, from the reaction mixture of Alendronate-Maleimide and peptide shows a chromatographic peak at 6.6min. (C) Mass spectrum of the chromatographic peak at 6.6min shows the mass/charge ratios of the peptide-ale (MW 1960), m/z 980.6, 654.1 and 490.8 of $2H^+$, $3H^+$ and $4H^+$ charges, respectively.

Substrate Fluorescence

Peptide

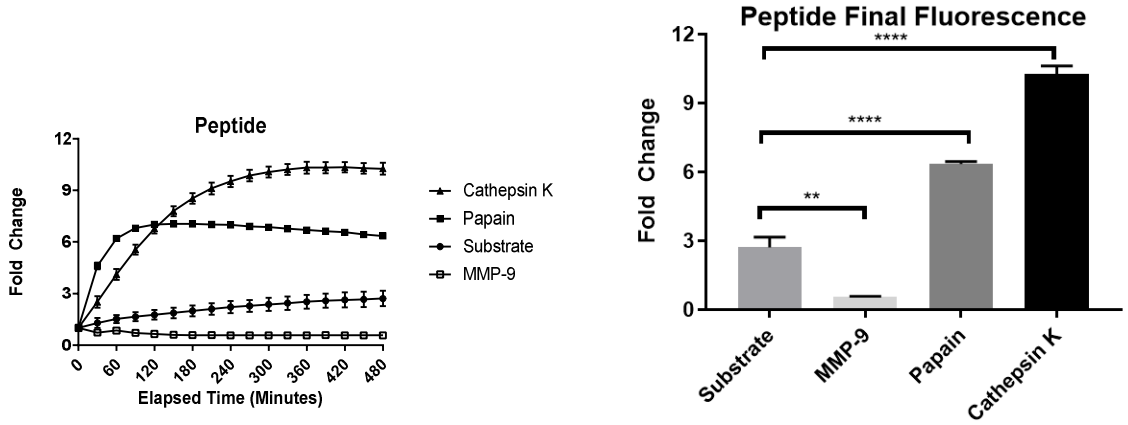

Figure 6 Fluorescence increase of incubation of non-conjugated peptide in the presence of papain, cathepsin K, MMP-9, or no enzyme in solution measured in a fluorescence plate reader. The second graph is the fold change of the final read compared to the initial baseline. n=4, error bars represent SEM.

In order to confirm specificity, the unconjugated commercially synthesized peptide was incubated with papain, Cathepsin K, MMP-9, and buffer. The final fold change in fluorescence after 8h as compared to a baseline read taken before addition of enzyme was 6.35 ± .10 for papain, 10.27 ± .355 for Cathepsin K, 0.58 ± .003 for MMP-9, and 2.71 ± .45 for the no enzyme control. Error is SEM with experiment replicated four times. Statistical analysis is by 2-way repeated measure ANOVA. Multiple comparisons for the main effect with columns, i.e. the enzyme, with Dunnett's multiple comparison test with the no enzyme control group as the control to which data is compared. All groups showed significant differences in column means from the no enzyme control ($p<.0001$ for papain and cathepsin K, $p=.0042$ for MMP-9). It is worth noting, however, that fluorescence for MMP-9 decreased for unknown reasons. Multiple comparisons are also done for the simple effect within columns, i.e. time. The value of the first read is compared to the value of all subsequent reads. For Cathepsin K and papain, all time points are significantly different are significantly different from the first read. For the no enzyme substrate, significance begins after an hour of incubation. However, the curve never plateaus like with papain and cathepsin K. For MMP-9, significance begins after two and a half hours, but fluorescence is decreasing.

Peptide-Ale

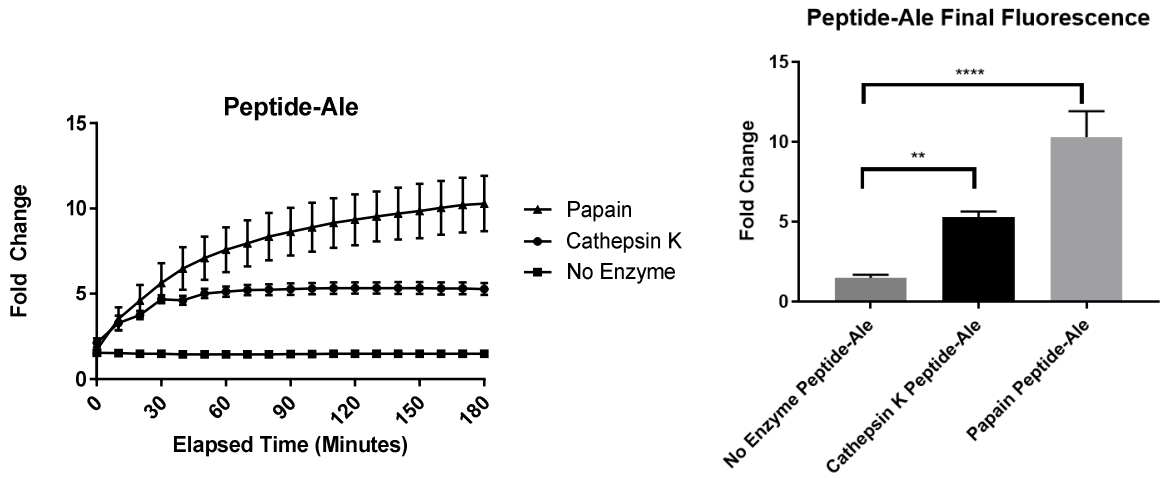

Figure 7 Fluorescence increase of incubation of conjugated peptide-Ale in the presence of papain, cathepsin K, or no enzyme in solution measured in a fluorescence plate reader. n=3, error bars represent SEM. The second graph shows the fold change of the final read compared to the initial baseline.

The peptide-Ale conjugate was incubated with papain, Cathepsin K, or buffer. The final fold change in fluorescence after 3h compared to a baseline read taken before enzyme was added was 10.29 ± 1.62 for papain, 5.29 ± .36 for Cathepsin K, and 1.49 ± .19 for buffer without enzyme. Error is SEM with experiment replicated three times. Statistical analysis is by 2-way repeated measure ANOVA (analysis of variance). Multiple comparisons are done for the main effect within columns, i.e. the effect of the enzyme, with Dunnett's multiple comparison test to the no enzyme control. Both groups showed significant differences in column means from the no enzyme control ($p=.0037$ for cathepsin k, $p<.0001$ for papain). Multiple comparisons are also done for the simple effect within columns, i.e. time, where the first read after addition of enzyme is the group to which the comparison is made. For Cathepsin K and papain, all rows are significantly different from the first row. For the no enzyme substrate, there is no significant difference for any row. We were not directly interested in quantified enzyme activity in these assays, so values like the V_{max} and the Michaelis constant were not calculated.

Peptide Binding

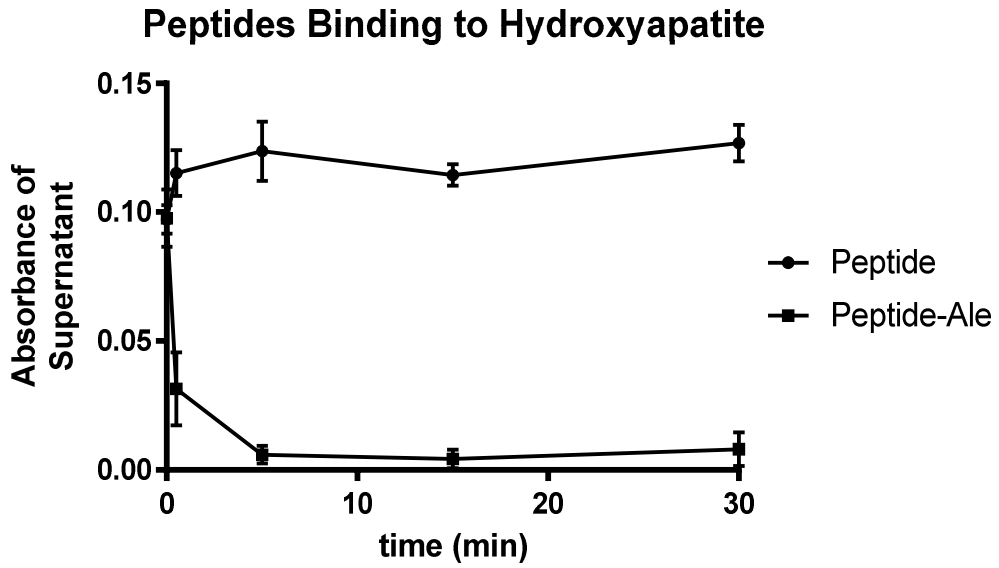

Figure 8 Absorbance of supernatant after incubation of unconjugated peptide and peptide-ale with hydroxyapatite beads. Absorbance quickly drops for peptide-Ale, indicating that it is being removed from the supernatant by binding to the hydroxyapatite beads. No such drop occurs for the unconjugated peptide.

The presence of peptide and peptide-Ale in the supernatant after incubation with hydroxyapatite, a form of calcium phosphate, powder is measured by UV absorbance in a plate reader. Peptide and peptide-Ale were incubated while shaking with hydroxyapatite powder in suspension, and supernatant was removed after centrifugation and the absorbance measured. This was to show firstly that absorbance dropped for peptide-Ale, indicating that it had bound to the hydroxyapatite and had been removed from the supernatant, and secondly to establish how quickly the binding occurred. The UV absorbance of the supernatant of the peptide-ale dropped to near zero within 5 minutes, while it remained stable for the peptide without alendronate, suggesting that the peptide-Ale, but not the peptide alone binds to hydroxyapatite. Binding saturation and the effect of dose were not directly investigated. Statistical analysis is by 2-way ANOVA.

Calcium Phosphate Plate Fluorescence

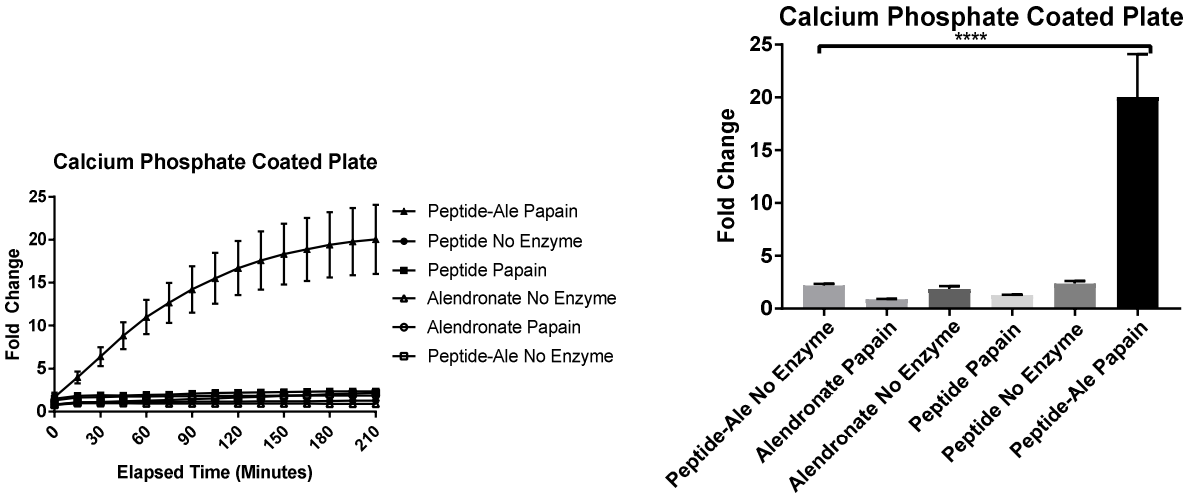

Figure 9 Fluorescence increase of incubation of conjugated peptide-ale, plain peptide, or alendronate alone in the presence of papain or no enzyme. Substrates are incubated for 5 minutes before washing and then washed three times. A baseline read is taken and then enzyme or vehicle is added. Fluorescence change is measured in a fluorescence plate reader. n=3, error bars represent SEM. The second graph is the final fold change in fluorescence from the initial baseline read.

The peptide, peptide-ale, and alendronate with no peptide were placed on a calcium phosphate coated plate which was then washed three times to remove any unbound substrate. We wanted to show that the peptide-Ale could still be cleaved when bound to the calcium phosphate surface and that only the peptide-Ale showed fluorescence, as we anticipated no fluorescence from alendronate alone and that the peptide without alendronate would be washed away. Papain or no enzyme was then added to the plate. Cathespin K is not active at neutral pH, and the acidic pH needed for activity dissolves the calcium phosphate. Thus, papain was used as a cathepsin K surrogate as it can cleave the peptide. The final fold change in fluorescence after 2.5h was 20.06 ± 4.04 for papain and peptide-Ale, 2.19 ± .137 for peptide-Ale with no enzyme, 2.36 ± .26 for peptide with no enzyme, 1.27 ± .05 for peptide and papain, 1.86 ± .28 for alendronate with no enzyme, and .91 ± .02 for alendronate with papain. Statistical analysis is by 2-way repeated measure ANOVA. Multiple comparisons for the main effect within columns, i.e. the combination of enzyme and peptide or alendronate, with Dunnett's multiple comparison test with the peptide-

ale with no enzyme control group as the control to which data is compared. Only the peptide-ale with papain group showed a significant difference, with $p<0.001$. Multiple comparisons are also done for the simple effect within columns, i.e. time, where the first read after addition of enzyme is the group to which the comparison is made. Only the peptide-ale with papain ever shows a significant difference from the first row, starting at 30 minutes.

Peptide Binding

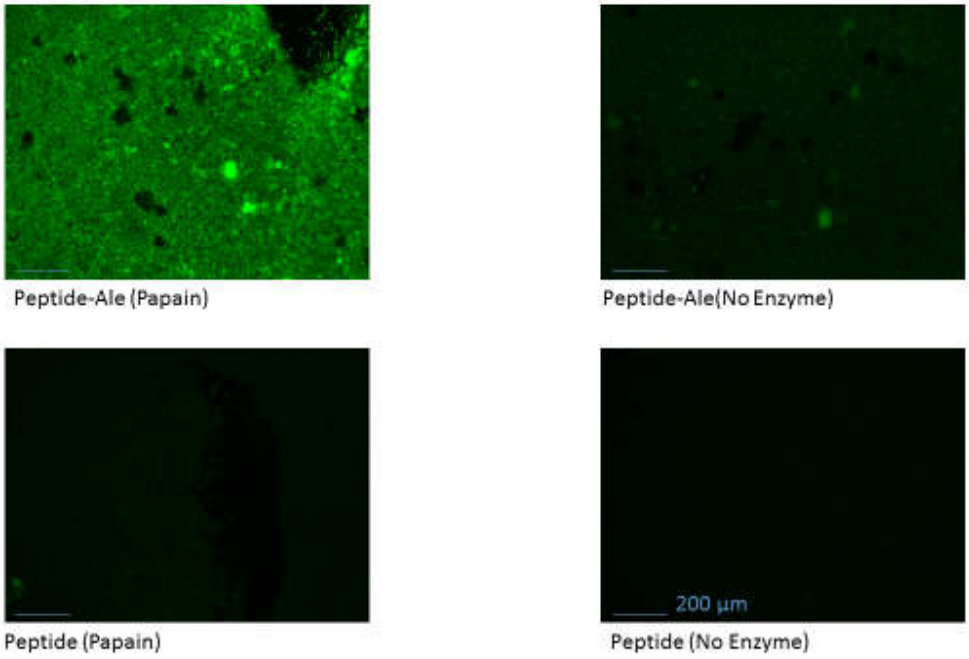

Figure 100 Images of a calcium phosphate plate incubated with peptide-ale or plain peptide with papain or no enzyme, similar to the experiment in Figure 7, but imaged instead of using a plate reader.

Figure 10 shows images of calcium phosphate-coated plates taken after the incubation experiment described above. Unconjugated peptide and peptide-Ale were given five minutes to bind and then washed three times before incubation with buffer or papain. Only peptide-Ale incubated with enzyme shows strong fluorescence. It is not surprising there is some fluorescence with peptide-Ale incubated without enzyme, because the quenching is not 100% efficient, so there is a small amount of baseline fluorescence. There is also a small amount of fluorescence

from the unconjugated peptide incubated with papain, possibly explained by non-specific peptide binding to the calcium phosphate surface.

Calcium Phosphate Plate Optimization

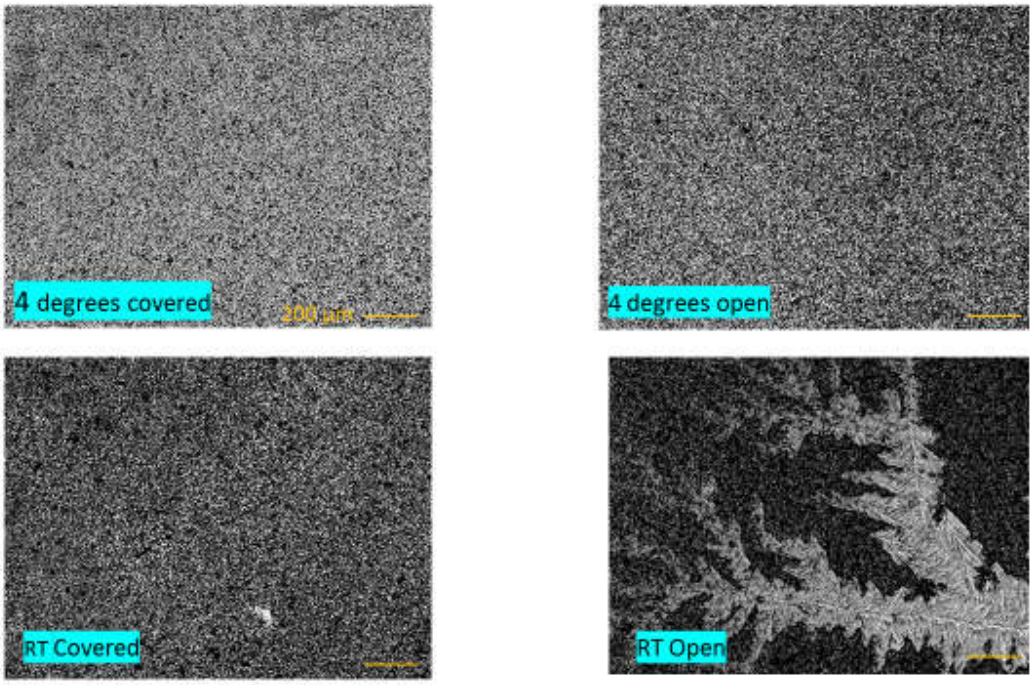

Figure 111 Brightfield imaging using the Operetta high content screening system results of different conditions for preparation of calcium-phosphate coated plates. Plates incubated at 4˚C covered or uncovered, and then at room temperature covered or uncovered. Scale bars are 200 µm.

Initially, the calcium phosphate coated plates were not able to support cell culture, though they were usable in biochemical assays. Cells failed to adhere and proliferate when seeded on plates following the initial Maria et. al protocol[35]. Our plates appeared to have a rougher surface than the previously published photos, so we hypothesized that our plates were too rough for the cells to adhere to. To solve this, the plate coating protocol was optimized. The same calcium and phosphate solutions were used but the incubation conditions were changed. Plates were covered or left open, and they were kept at room temperature or 4˚C. All four conditions had a visible calcium phosphate coating. The plates were then imaged using the Operetta imaging system,

using only the brightfield, which is the same system used for fluorescence imaging of the cells. The 4˚C covered plate appeared to have the smoothest surface, so it was then used in cell culture. Cells could adhere and proliferate, so the protocol was adapted to include refrigeration of covered 96 well plates.

Osteoclast Generation

Successfully culturing osteoclasts proved to be the most difficult part of this project. The first trial to grow osteoclasts from RAW 264.7 monocytes on a standard, sterile 96-well culture plate was successful, which is indicated by the formation of large cells with three or more nuclei that are positive for TRAP when stained. Figure 12 shows images of RAW 264.7 incubated with the differentiation factor RANKL for 2 (left) or 4 days (right). After 2 days, the cells are mainly still mononucleated monocytes, as opposed to a four-day incubation where a large, multinucleated cell has formed. The purple-red TRAP staining indicates formation of osteoclasts.

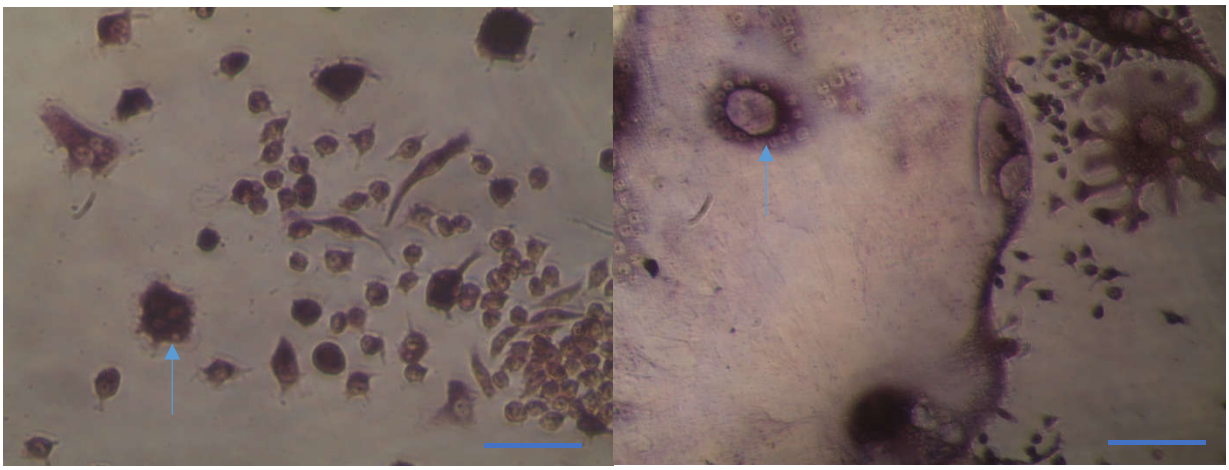

Figure 12 Sample RAW 264.7 cell culture. Cells on the left were incubated for two days with RANKL and without RANKL for the following two days. Cells on the right were incubated for four days with RANKL. The cells were fixed and stained for TRAP. Blue arrows indicate a sample TRAP positive area. Scalebars are 100 µm.

Despite initial successful results, the culture was unreliable and irreproducible. Figure 13 shows an unsuccessful attempt where monocytes failed to differentiate after 6 days of incubation with

RANKL. The inability of the RAW 264.7 monocytes to grow was largely solved by changing the calcium phosphate coating protocol.

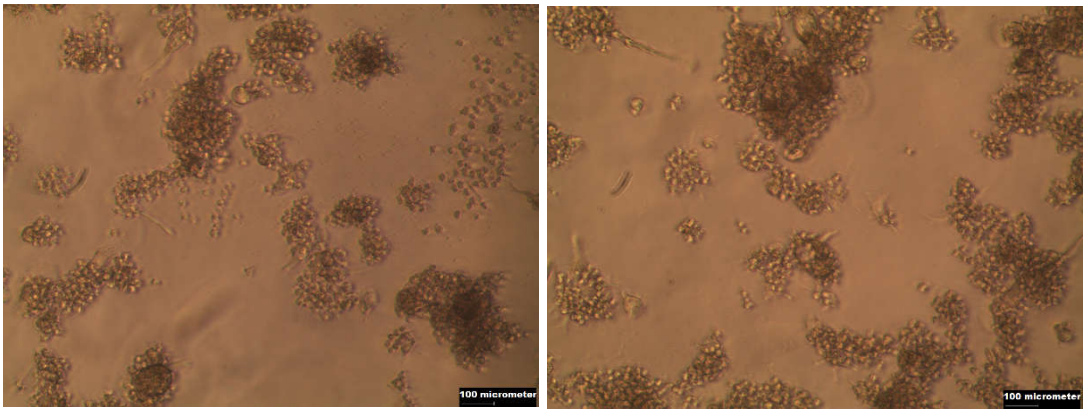

Figure 13 RAW 264.7 cells that failed to differentiate into multinucleated osteoclasts. Two days of RANKL on the left, and eight days of RANKL on the right.

However, this was only part of the problem. Even on a standard culture plate without calcium phosphate coating, osteoclasts failed to form. Pictured (Figure 13) is an example after 8 days of culture, with a negative control on the left and a positive control on the right. No large, multinucleated cells have formed.

To attempt to solve this problem, many different things were tried. Cells were seeded at 1000, 1500, and 2000 cells per well were seeded. Higher densities result in confluent monocytes that were unable to differentiate. Different concentrations of RANKL (25, 50, and 100 µg/mL) were also used but did not result in major differences on both normal and calcium phosphate-coated 96-well plates. We suspected that the main variable could be the RANKL. Since monocytes rarely failed to grow, the media and sterilization of the plates was not questioned. But since RANKL is absolutely necessary for osteoclastogenesis, faulty RANKL would result in no formation of osteoclasts. Various aliquots and lots of recombinant RANKL from the lab of Dr. Svetlana Komarova were used, with mixed results where sometimes a culture would work

sometimes would fail under the same initial conditions. We then switched to commercial recombinant RANKL from Peprotech, which gave more reproducible results.

Fluorescence Imaging

5 days RANKL (osteoclasts) 2 days RANKL (monocytes)

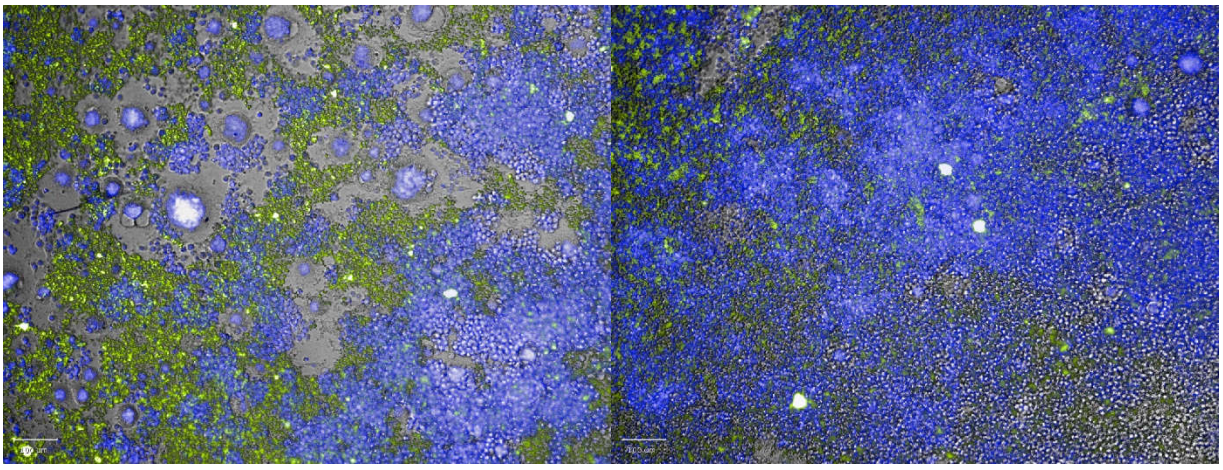

Above: 24 hours of peptide-ale incubation.

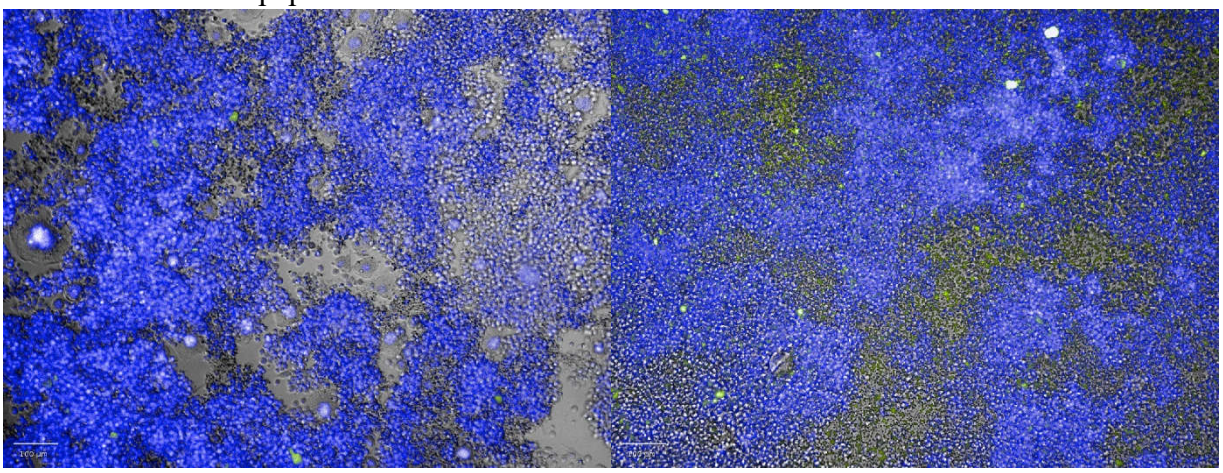

Above: 5 minutes of incubation with peptide-ale.

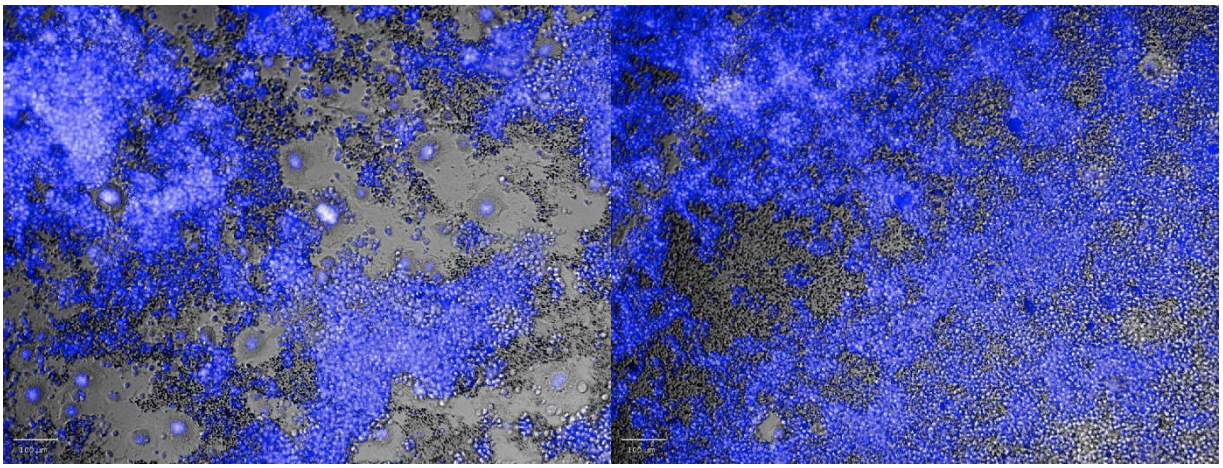

Above: no addition of peptide-ale.

Figure 14 Fluorescent images of osteoclast and monocyte cultures. Left column is five days of incubation with RANKL forming multinucleated osteoclasts, and the right column is two days of RANKL followed by two days without. Top row is 24h of incubation with peptide-ale, the middle row is 5 minutes of incubation, and the bottom row is no probe added.

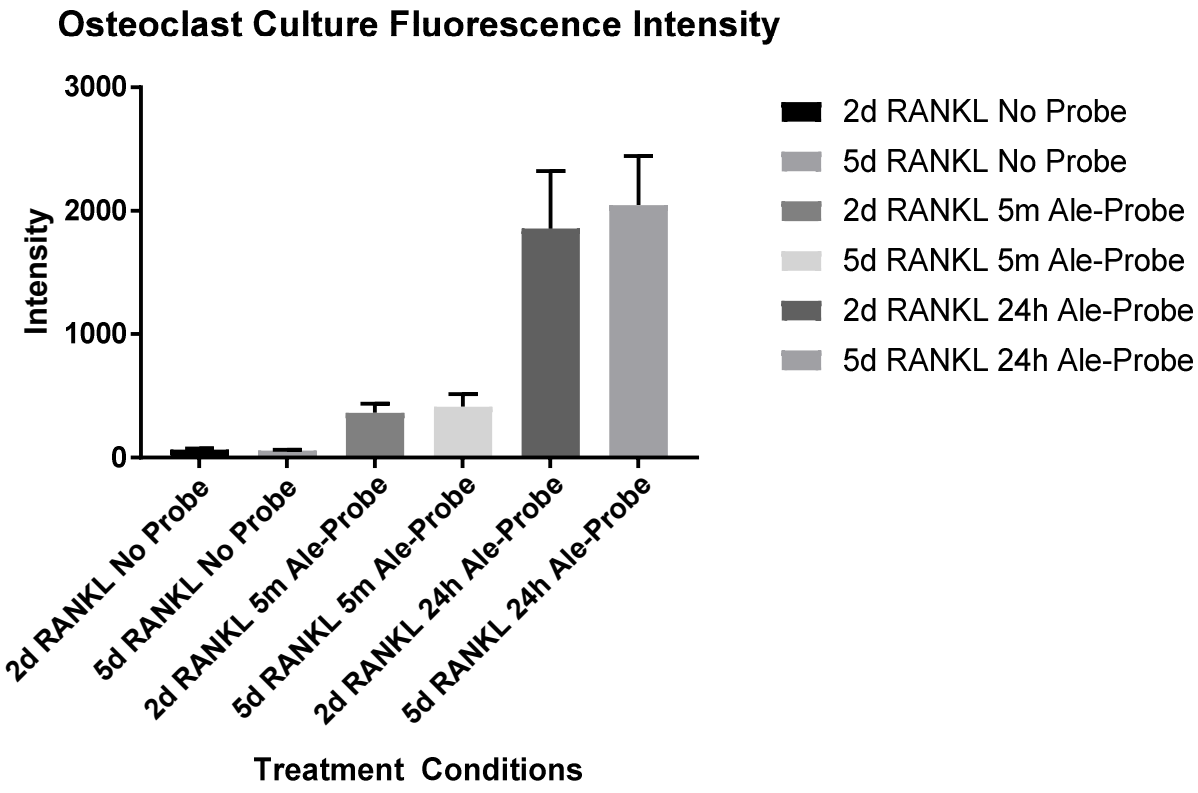

Figure 15 Quantification of above images. Analysis by one-way ANOVA with Tukey's post-hoc test. $p < .0001$, $n=8$.

RAW cells were incubated for four to six days, indicated as the average of 5 days in the above images and graphs, depending on when multinucleated cells formed. For a negative control, RAW cells were incubated with RANKL only for the two initial days, and for osteoclast

formation cells were exposed to RANKL for the entire culture period. The peptide-ale probe was added to living cells. After incubation with the peptide-ale for twenty-four hours or five minutes on a calcium phosphate coated plate, cell cultures were fixed with formalin, stained with Hoechst, and imaged using the Operetta high content screening system (Figure 14). The fluorescence intensity of the green fluorescein of the overall image was then quantified. When no probe is added, very little fluorescence is seen in monocyte or osteoclast culture. When probe is added for five minutes, where it has time to bind to the calcium phosphate but little exposure to cathepsin K for cleavage, fluorescence increases somewhat which is expected as the quenching is not 100% efficient. After incubation with peptide-ale for 24 hours, fluorescence increases approximately five folds from the probe only incubated for five-minutes (Figure 15). There is a statistically significant difference between no probe and five minutes of probe from the 24-hour probe incubation. However, there is no significant difference observed between monocyte and osteoclast culture, suggesting there is cathepsin K expressed by the monocytes as well.

Discussion

Cathepsin K is the most important enzyme in the breakdown of bone. This project is a proof-of-principle that a bisphosphonate-bound fluorogenic probe could be used as a tool to study cathepsin K activity in mineralized tissues. Cathepsin K is well known to be highly expressed in mature osteoclasts in order to break down the organic collagen matrix, so it was possible to use mature osteoclasts as an *in vitro* model of the probe activity. However, it was necessary to have a biomimetic surface of bone, namely the calcium phosphate mineral, in order to demonstrate the bone-binding properties of our probe. To do so, a previously published method with some of our modifications was used.[35]

But before cell culture, it was necessary to establish that the probe had actually been synthesized and was useful, using chemical and biochemical methods. The probe was synthesized in a two-step process, in which alendronate was conjugated to a maleimide, and a second step where a fluorescent peptide with a cysteine residue was conjugated to the alendronate-maleimide. In both cases, the synthesis of the desired product was straightforward, but the purification steps were more challenging. Ultimately, reverse-phase chromatography proved to be successful in purifying the material.

Fluorescence and Possible Improvements

While the purification and syntheses were being optimized, biochemical experiments using purified enzyme and probe were conducted. Before using cells, we wanted to ensure that enzymatic cleavage of our substrates was possible. Though based on previous studies[30, 32], we wanted to verify that our substrates could be cleaved. In previous studies, different sets of dye-quencher pairs were used. In addition, the conjugation to alendronate was an innovation, and we need to ensure that the alendronate did not prohibit cleavage. Generally, we observed a roughly five-fold increase in fluorescence after incubation with enzyme, either in a fluorescence microplate reader or in cell culture. Though this is sufficient for proof-of-principle, in an *in vivo* model it would be preferable to use a dye-quencher pair with a higher quenching efficiency in order to have an increased dynamic range, for example coumarin and QSY-7 instead of fluorescein and dabcyl.[36] In addition, it would be better to use near-infrared dyes because of the relatively high penetrance of near infrared right into tissue, especially important for deep tissues like some bones, and the lower autofluorescence in the NIR range.[29] This allows for whole, live animal imaging whereas for a probe like ours, it would be necessary to take sections of a sacrificed animal, or isolate tissues.[29]

Osteoclast Cultures

Culture of osteoclasts on calcium phosphate-coated plates proved difficult. The formation of osteoclasts was found through trial and error to be very sensitive to the initial seeding conditions. Seeding too many cells resulted in the formation of confluent monocytes with no osteoclasts, while seeding too few cells resulted in clumps of monocytes, again without osteoclasts. Often, the core of the clumps would have dead cells in them. Between 1500-2000 cells per well in a 96 well plate, or 4500-6000 per cm^2 were found to be ideal densities however it varies somewhat depending on the calcium phosphate coating. Some coatings were rougher and required slightly higher densities, and smoother coatings needed fewer cells.

The first sets of calcium phosphate coated plates had no cell growth at all. Monocytes would be seeded, but after a few days few to no cells would survive. The first thing tried to fix this was changing the protocol to have no media change. This was based on the thought that maybe cells were not attaching well to the surface and were being aspirated off during the media change. However, this failed to affect the outcome. The next thing tried was a test of different methods of coating the plates, as described in methods. From this, the plate that appeared to have the smoothest surface after a simple visual inspection was seeded, and monocytes were able to grow even though osteoclasts did not immediately form.

An ongoing problem with the cell culture after designing a calcium phosphate plate protocol cells grew on was that formation of osteoclasts was inconsistent. This indicated that the basic protocol was working, but there was something subtly different between replicates that resulted in different results. Though it is impossible to determine exactly what that difference was, a few things were observed over time. First, is that cells prefer fresh media. After about a month, even if the pH of the media is good and there is no contamination, the cells were less

likely to form osteoclasts. They are also sensitive to the FBS (fetal bovine serum). It appears that sometimes a particular lot of FBS does not support the growth of osteoclasts. Third, the RANKL used is critically important. If the RANKL has expired or the dosage is wrong, osteoclasts will not form. The calcium phosphate is also crucial. If the surface is too rough, osteoclasts will not form. Though this was never directly quantified, osteoclasts grown on polystyrene tissue-culture treated plates were generally larger than the ones grown on calcium phosphate.

Once osteoclasts had formed, the peptide-ale was added to both the osteoclasts and monocytes. After incubation, the cells were fixed, Hoechst DNA stain added, and then imaged and quantified. The use of the Operetta high content screening imaging system (Perkin Elmer) was chosen for two reasons: ease of quantification with the Columbus analysis software and reduced exposure to light, e.g. lessened time to focus images, to reduce the effect of photobleaching.

Failure of the Monocyte Negative Control

After quantification of images (Figure 15), it was apparent that that one of the negative controls had failed. When no peptide-ale was added to control for background autofluorescence, or when peptide-ale was added and fixed after five minutes, there was a significant difference from when cells were incubated with peptide-ale for 24 hours. However, there was no difference between when cells had been incubated with RANKL for the first two days after seeding and when cells had been exposed to RANKL the entire culture time. There are two plausible explanations for this. One, that simple exposure to the cells caused the fluorescence increase. Two, that cathepsin K was also being expressed by the monocytes. Because it has been previously shown that cell lysates from a cathepsin K knockout mouse were unable to cleave a very similar substrate[30], it seems more likely that the monocytes were also expressing cathepsin

K. Indeed, it has been shown that monocytes exposed to RANKL produce cathepsin K even before osteoclasts are formed.[37]

To remedy this problem, a few solutions are proposed. First is to culture monocytes with no exposure to RANKL at all. The purpose of initial exposure to RANKL is to prime the cells for osteoclast formation. This starts the cells expressing osteoclast related genes, e.g. Cathepsin K and TRAP, but multinucleated cells do not form. [34] We expected that these cells would express low levels of Cathepsin K and we would see a lower fluorescence than in mature osteoclasts, though our measurement method was unable to detect a difference. The literature suggests that the RAW 264.7 monocytes were producing cathepsin K,[37] though we did not check expression levels using Western blotting or RT-PCR which can be done quantitatively. Secondly, more timepoints will be added to see how fluorescence increases with time when not all of the peptide-ale substrate has been cleaved. Something similar could be accomplished using live cell imaging over time. Thirdly, black optical bottom plates will be used to reduce fluorescence crosstalk between wells on the clear plates previously being used.

Future Directions

A very similar probe could be made using near-infrared dyes for use in live animals as mentioned previously, by switching our dye and quencher for near-infrared dyes and quencher, for example donor IRDye 800CW (Lidor) and quencher QC1.[38] Or, the amino sequence could be changed so that the probe is specific for another enzyme. For example, Pro-Arg-(Ser/Thr)-↓-(Leu/Ile)-(Ser/Thr) is the ideal cleavage sequence for MMP-9,[39] which is involved in the migration of osteoclasts, with the cleavage site indicated by the arrow. Proteases expressed by cancer cells believed to be involved in cancer metastases to the bone could also be investigated if a specific amino acid cleavage site exists.

In conclusion, we have successfully synthesized an alendronate-conjugated fluorescent peptide with specificity for cathepsin K. We have shown that the substrate can be cleaved with purified Cathepsin K as well as a non-mammalian positive control. *In vitro* we have shown that after exposure to cells we see a fluorescence increase over baseline values with no probe at all for background fluorescence as well as when the probe was added but not given time to be cleaved. We will continue to add more time points as well as use as a Cathepsin K inhibitor, namely odanacatib, in order to more convincingly show that the *in vitro* cleavage is indeed done by Cathepsin K.

However, there are still limitations to this system. The probe is not ratiometric, as we are not able to quantify the fluorescence of each fluorophore independently. Ratiometric probes are concentration independent, where the wavelengths of two fluorescence substrates, e.g. quantum or carbon dots, are read in quick session and the ratio of the intensities of the two is the output. With our dye-quencher system, the fluorescence depends on the concentration of the probe present which is not feasible to calculate to the precision and accuracy needed on a bone surface *in vivo*. If a site has more probe even if a smaller fraction has been dequenched than at another site with more dequenching yet less probe, it may still give a higher signal. Therefore, it can be difficult to compare results across experiments and replicates, though normalization and controls help avoid this problem. A second limitation is the choice of dye, fluorescein. It fluoresces in the green range and is prone to photobleaching. Especially because we want to image bone, often a tissue deep into the body, the high autofluorescence of tissues in the green wavelengths and low penetration of the excitation wavelength in this range means the probe is not suitable for live *in vivo* imaging. *In vivo* imaging could be done, but it would have to be on a sacrificed and dissected animal.

To avoid this problem, a near-infrared dye and quencher pair could have been used. There is much deeper penetration into tissue and lower autofluorescence in the near infrared range [29]. Both the concentration-dependency of our probe and the inability to do *in vivo* live imaging could have been ameliorated using a ratiometric NIR nanoparticles, most likely custom-designed carbon dots. However, near-infrared imaging requires specialized equipment compared to the green filter sets used for GFP and fluorescein, which are ubiquitous in fluorescence microscopes and plate readers. Also, ratiometric imaging and measurements requires that the instrumentation be able to switch between reading two different wavelengths very quickly, which not all equipment is able to do. Secondly, both near-infrared non-ratiometric dyes and especially ratiometric nanoparticles are substantially more expensive than the relatively inexpensive fluorescein and dabcyl dye-quencher pair. For a proof-of-principle project for use in biochemical and *in vitro* cell culture assays, the green fluorescence is sufficient.

References

1. Paiva, K. B.; Granjeiro, J. M., Bone tissue remodeling and development: focus on matrix metalloproteinase functions. *Arch Biochem Biophys* **2014,** *561*, 74-87.
2. Cappariello, A.; Maurizi, A.; Veeriah, V.; Teti, A., Reprint of: The Great Beauty of the osteoclast. *Archives of Biochemistry and Biophysics* **2014,** *561* (0), 13-21.
3. Lacey, D. L.; Timms, E.; Tan, H. L.; Kelley, M. J.; Dunstan, C. R.; Burgess, T.; Elliott, R.; Colombero, A.; Elliott, G.; Scully, S.; Hsu, H.; Sullivan, J.; Hawkins, N.; Davy, E.; Capparelli, C.; Eli, A.; Qian, Y. X.; Kaufman, S.; Sarosi, I.; Shalhoub, V.; Senaldi, G.; Guo, J.; Delaney, J.; Boyle, W. J., Osteoprotegerin Ligand Is a Cytokine that Regulates Osteoclast Differentiation and Activation. *Cell* **1998,** *93* (2), 165-176.
4. Boyle, W. J.; Simonet, W. S.; Lacey, D. L., Osteoclast differentiation and activation. *Nature* **2003,** *423* (6937), 337-342.
5. Supanchart, C.; Kornak, U., Ion channels and transporters in osteoclasts. *Archives of Biochemistry and Biophysics* **2008,** *473* (2), 161-165.
6. Okada, Y.; Naka, K.; Kawamura, K.; Matsumoto, T.; Nakanishi, I.; Fujimoto, N.; Sato, H.; Seiki, M., Localization of matrix metalloproteinase 9 (92-kilodalton gelatinase/type IV collagenase = gelatinase B) in osteoclasts: Implications for bone resorption. *Laboratory Investigation* **1995,** *72* (3), 311-322.

7. Mosig, R. A.; Dowling, O.; DiFeo, A.; Ramirez, M. C. M.; Parker, I. C.; Abe, E.; Diouri, J.; Al Aqeel, A.; Wylie, J. D.; Oblander, S. A.; Madri, J.; Bianco, P.; Apte, S. S.; Zaidi, M.; Doty, S. B.; Majeska, R. J.; Schaffler, M. B.; Martignetti, J. A., Loss of MMP-2 disrupts skeletal and craniofacial development and results in decreased bone mineralization, joint erosion and defects in osteoblast and osteoclast growth. *Human Molecular Genetics* **2007,** *16* (9), 1113-1123.
8. Andersen, T. L.; Del Carmen Ovejero, M.; Kirkegaard, T.; Lenhard, T.; Foged, N. T.; Delaissé, J. M., A scrutiny of matrix metalloproteinases in osteoclasts: Evidence for heterogeneity and for the presence of MMPs synthesized by other cells. *Bone* **2004,** *35* (5), 1107-1119.
9. Bromme, D.; Okamoto, K.; Wang, B. B.; Biroc, S., Human cathepsin O2, a matrix protein-degrading cysteine protease expressed in osteoclasts. Functional expression of human cathepsin O2 in Spodoptera frugiperda and characterization of the enzyme. *J Biol Chem* **1996,** *271* (4), 2126-32.
10. Littlewood-Evans, A.; Kokubo, T.; Ishibashi, O.; Inaoka, T.; Wlodarski, B.; Gallagher, J. A.; Bilbe, G., Localization of cathepsin K in human osteoclasts by in situ hybridization and immunohistochemistry. *Bone* **1997,** *20* (2), 81-6.
11. Gelb, B. D.; Shi, G. P.; Chapman, H. A.; Desnick, R. J., Pycnodysostosis, a lysosomal disease caused by cathepsin K deficiency. *Science* **1996,** *273* (5279), 1236-8.
12. Zhao, B.; Janson, C. A.; Amegadzie, B. Y.; D'Alessio, K.; Griffin, C.; Hanning, C. R.; Jones, C.; Kurdyla, J.; McQueney, M.; Qiu, X.; Smith, W. W.; Abdel-Meguid, S. S., Crystal structure of human osteoclast cathepsin K complex with E-64. *Nature structural biology* **1997,** *4* (2), 109-11.
13. Novinec, M.; Lenarcic, B., Cathepsin K: a unique collagenolytic cysteine peptidase. *Biol Chem* **2013,** *394* (9), 1163-79.
14. Franchi, A., Epidemiology and classification of bone tumors. *Clinical Cases in Mineral and Bone Metabolism* **2012,** *9* (2), 92-95.
15. Li, S.; Peng, Y.; Weinhandl, E. D.; Blaes, A. H.; Cetin, K.; Chia, V. M.; Stryker, S.; Pinzone, J. J.; Acquavella, J. F.; Arneson, T. J., Estimated number of prevalent cases of metastatic bone disease in the US adult population. *Clinical Epidemiology* **2012,** *4*, 87-93.
16. Gauthier, J. Y.; Chauret, N.; Cromlish, W.; Desmarais, S.; Duong, L. T.; Falgueyret, J. P.; Kimmel, D. B.; Lamontagne, S.; Leger, S.; LeRiche, T.; Li, C. S.; Masse, F.; McKay, D. J.; Nicoll-Griffith, D. A.; Oballa, R. M.; Palmer, J. T.; Percival, M. D.; Riendeau, D.; Robichaud, J.; Rodan, G. A.; Rodan, S. B.; Seto, C.; Therien, M.; Truong, V. L.; Venuti, M. C.; Wesolowski, G.; Young, R. N.; Zamboni, R.; Black, W. C., The discovery of odanacatib (MK-0822), a selective inhibitor of cathepsin K. *Bioorg Med Chem Lett* **2008,** *18* (3), 923-8.
17. Merck, Merck Provides Update on Odanacatib Development Program. 2016.
18. Cremers, S. C. L. M.; Pillai, G.; Papapoulos, S. E., Pharmacokinetics/Pharmacodynamics of Bisphosphonates. *Clinical Pharmacokinetics* **2005,** *44* (6), 551-570.
19. van Beek, E. R.; Cohen, L. H.; Leroy, I. M.; Ebetino, F. H.; Lowik, C. W.; Papapoulos, S. E., Differentiating the mechanisms of antiresorptive action of nitrogen containing bisphosphonates. *Bone* **2003,** *33* (5), 805-11.
20. Luckman, S. P.; Hughes, D. E.; Coxon, F. P.; Graham, R.; Russell, G.; Rogers, M. J., Nitrogen-containing bisphosphonates inhibit the mevalonate pathway and prevent post-translational prenylation of GTP-binding proteins, including Ras. *J Bone Miner Res* **1998,** *13* (4), 581-9.

21. Sobel, S., Center for Drug Evaluation and Research Approval Package for Application Number 020560, S015. Administration, F. a. D., Ed. Rockville, MD, 1999.
22. Coskun Benlidayi, I.; Guzel, R., Oral Bisphosphonate Related Osteonecrosis of the Jaw: A Challenging Adverse Effect. *ISRN Rheumatology* **2013,** *2013*, 215034.
23. Sabatino, R.; Antonelli, A.; Battistelli, S.; Schwendener, R.; Magnani, M.; Rossi, L., Macrophage Depletion by Free Bisphosphonates and Zoledronate-Loaded Red Blood Cells. *PLOS ONE* **2014,** *9* (6), e101260.
24. Ferreira Ddos, S.; Boratto, F. A.; Cardoso, V. N.; Serakides, R.; Fernandes, S. O.; Ferreira, L. A.; Oliveira, M. C., Alendronate-coated long-circulating liposomes containing 99mtechnetium-ceftizoxime used to identify osteomyelitis. *Int J Nanomedicine* **2015,** *10*, 2441-50.
25. Giger, E. V.; Castagner, B.; Leroux, J.-C., Biomedical applications of bisphosphonates. *Journal of Controlled Release* **2013,** *167* (2), 175-188.
26. Zaheer, A.; Lenkinski, R. E.; Mahmood, A.; Jones, A. G.; Cantley, L. C.; Frangioni, J. V., In vivo near-infrared fluorescence imaging of osteoblastic activity. *Nature Biotechnology* **2001,** *19*, 1148.
27. Fogelman, I., The Bone Scan—Historical Aspects. In *Bone Scanning in Clinical Practice*, Fogelman, I., Ed. Springer London: London, 1987; pp 1-6.
28. Lavis, L. D.; Raines, R. T., Bright Building Blocks for Chemical Biology. *ACS Chemical Biology* **2014,** *9* (4), 855-866.
29. Zhang, X.; Bloch, S.; Akers, W.; Achilefu, S., Near-infrared Molecular Probes for In Vivo Imaging. *Current Protocols in Cytometry* **2012,** *CHAPTER*, Unit12.27-Unit12.27.
30. Lecaille, F.; Weidauer, E.; Juliano, M.; Bromme, D.; Lalmanach, G., Probing cathepsin K activity with a selective substrate spanning its active site. *Biochem. J* **2003,** *375*, 307-312.
31. Alvarado-Gonzalez, M.; Gallo, M.; Lopez-Albarran, P.; Flores-Holguin, N.; Glossman-Mitnik, D., DFT study of the interaction between the conjugated fluorescein and dabcyl system, using fluorescene quenching method. *J Mol Model* **2012,** *18* (9), 4113-20.
32. Jaffer, F. A.; Kim, D. E.; Quinti, L.; Tung, C. H.; Aikawa, E.; Pande, A. N.; Kohler, R. H.; Shi, G. P.; Libby, P.; Weissleder, R., Optical visualization of cathepsin K activity in atherosclerosis with a novel, protease-activatable fluorescence sensor. *Circulation* **2007,** *115* (17), 2292-8.
33. Hermanson, G. T., Chapter 19 - Vaccines and Immunogen Conjugates. In *Bioconjugate Techniques (Third edition)*, Hermanson, G. T., Ed. Academic Press: Boston, 2013; pp 839-865.
34. Tiedemann, K.; Hussein, O.; Sadvakassova, G.; Guo, Y.; Siegel, P. M.; Komarova, S. V., Breast cancer derived factors stimulate osteoclastogenesis through the Ca2+ /PKC and TGFβ/MAPK signaling pathways. *Journal of Biological Chemistry* **2009**.
35. Maria, S. M.; Prukner, C.; Sheikh, Z.; Mueller, F.; Barralet, J. E.; Komarova, S. V., Reproducible quantification of osteoclastic activity: characterization of a biomimetic calcium phosphate assay. *Journal of biomedical materials research. Part B, Applied biomaterials* **2014,** *102* (5), 903-12.
36. Marras, S. A. E.; Kramer, F. R.; Tyagi, S., Efficiencies of fluorescence resonance energy transfer and contact-mediated quenching in oligonucleotide probes. *Nucleic acids research* **2002,** *30* (21), e122-e122.
37. Pang, M.; Martinez, A. F.; Fernandez, I.; Balkan, W.; Troen, B. R., AP-1 stimulates the cathepsin K promoter in RAW 264.7 cells. *Gene* **2007,** *403* (1), 151-158.

38. Peng, X.; Draney, D. R.; Volcheck, W. M. In *Quenched near-infrared fluorescent peptide substrate for HIV-1 protease assay*, SPIE BiOS, SPIE: 2006; p 12.
39. Kridel, S. J.; Chen, E.; Kotra, L. P.; Howard, E. W.; Mobashery, S.; Smith, J. W., Substrate Hydrolysis by Matrix Metalloproteinase-9*. *Journal of Biological Chemistry* **2001,** *276* (23), 20572-20578.